Microstructural evolution/durability of magnesium phosphate cement paste over time in neutral and basic environments

Hugo Lahalle, Cédric Patapy, Marwa Glid, Guillaume Renaudin, Martin Cyr

Microstructural evolution / durability of magnesium phosphate cement paste over time in neutral and basic environments.

Hugo LAHALLE [1*], Cédric PATAPY [1], Marwa GLID [2], Guillaume RENAUDIN [2], Martin Cyr [1]

1. LMDC, Université de Toulouse, INSA/UPS Génie Civil, 135 Avenue de Rangueil, 31077 Toulouse cedex 04 France.

2. Université Clermont Auvergne, CNRS, SIGMA Clermont, ICCF, F-63 000 Clermont-Ferrand, France.

Abstract

This study investigates the evolutions of the mineralogy, pore solution and porosity of magnesium potassium phosphate cement pastes (MKPC) over time in neutral and basic environments, media that MKPC pastes might encounter when used as patch repair materials or as stabilization materials for hazardous wastes. Mineralogy evolutions were characterized by X-ray diffraction/Rietveld (XRD) and thermogravimetric analyses (TGA) and completed with scanning electron microscopy (SEM/EDX) microanalyses. Pore solution compositions (ICP-OES, IC) and the porosity of the materials were also analyzed. The results showed an amorphization of MKPC pastes over time that might be related to structural changes for the K-struvite phase. Achieving chemical equilibrium between the cementitious waters and the MKPC pore solution can result in porosity evolutions within the materials. Transport and mechanical changes might be expected, especially for MKPC pastes kept in basic media, since K-struvite [$MgKPO_4.6H_2O$], could be partially dissolved, leading to a higher total pore volume.

Keywords:

B: crystal structure; B: pore solution; C: aging; C: durability; D: chemically-bonded ceramics

[*] **Corresponding author: lahalle@insa-toulouse.fr (additional email address: hugo.lahalle@hotmail.com),**

1. Introduction

Magnesium phosphate cements (MPCs) or chemically bonded ceramics [1,2] result from an acid-base reaction between hard-burnt magnesia (MgO) and a water-soluble phosphate salt ($(NH_4)_2HPO_4$, $(NH_4)H_2PO_4$, or KH_2PO_4) [3,4]. They have been attracting more and more attention over recent decades as alternatives to conventional cementitious materials for special binder applications. Their fast setting and hardening, their good volume stability and their high bonding strength make them ideal for rapid repair work [5-7]. MPCs are also arousing increasing interest in the field of hazardous (e.g. toxic or radioactive) waste stabilization/solidification [8-20], and in biomedical applications [21-23].

Lately, ammonium salts ($(NH_4)_2HPO_4$, $(NH_4)H_2PO_4$) have tended to be replaced by potassium salt (KH_2PO_4) to avoid the release of noxious ammonia that can occur during the setting and hardening process [2, 3]. Potassium salt is used preferentially since it yields materials with higher mechanical strength. The major hydration product is then K-struvite ($MgKPO_4.6H_2O$) (Eq.1).

$$MgO + KH_2PO_4 + 5H_2O \rightarrow MgKPO_4.6H_2O \quad \text{(Eq.1)}$$

Several research works have been carried out on magnesium potassium phosphate cements (MKPCs) for Mg/P molar ratios ranging from 1 to 14 and water to cement weight ratios ranging from 0.11 to 100. Most of the studies deal with the hydration process, which is more complex than is suggested by the mass balance equation (1) [24-29], and mechanical properties [30-38]. However there are few papers assessing the durability of the materials, which is essential information when new materials are created or existing ones are improved. These few studies carried out on magnesium phosphate cement with low water to cement weight ratios, and thus residual MgO and/or KH_2PO_4, have shown the evolution of the mechanical and transport properties of magnesium phosphate cement over time in contact with aqueous solutions (most of the time in water). Yang et al. [39] showed that magnesium ammonium phosphate mortars (Mg/P molar ratio of 3 and water to cement weight ratio of 0.44) lost 10 % and 18 % of their compressive strength for samples immersed in water for 28 days and 90 days respectively. The same trend was observed by Li and Chen [40] for magnesium potassium phosphate cement mortars immersed in water (18 % loss after 90 days of immersion). Wang et al. [41] highlighted that the alkali resistance

of MPC mortars was poor and might be closely related to the stability of the hydration product $MgNH_4PO_4.6H_2O$ (struvite). Recently, Le Rouzic [42] et al. studied the durability of MKPC pastes ($MgO + KH_2PO_4$) for Mg/P molar ratios ranging from 1 to 10 and water to binder weight ratio of 0.2. They showed that low Mg/P molar ratio (Mg/P < 5) led to residual KH_2PO_4 and thus to efflorescence, poor water resistance, swelling and cracking. These phenomena were also observed by other authors when an excess of KH_2PO_4 remained in the porosity of the material [40, 43-44]. In addition, some questions have arisen concerning the long-term evolution of such materials, which contain unreacted MgO, in a humid environment [45]it is known that hydration of MgO into $Mg(OH)_2$ is accompanied by a significant volume increase (by 118%), which can induce notable expansion in hardened cement-based materials [46, 47].

The present study aims to assess the microstructural behavior of magnesium potassium phosphate cements (MKPCs) over time when they are in contact with neutral and basic environments - environments that might be encountered when such cements are used as repair materials or for conditioning nuclear wastes. Mineralogical, pore solution and porosity changes that could occur in the material have barely been investigated up to now. The MKPC paste studied in the present work was developed by CEA (LCBC) for the stabilization/solidification of aluminum metal [19] and presents the advantage of having good mechanical properties, good workability and very low residual MgO and KH_2PO_4, since an Mg/P molar ratio of 1 is used, together with a water to cement weight ratio of 0.56, which is close the chemical water demand of the cement (w/c = 0.51). Small monolithic samples and crushed powder were used in order to speed up possible mineralogical and pore solution changes, and the porosity of the samples was also studied by mercury intrusion porosimetry using an appropriate drying method for MKPCs. These accelerated tests carried out over six months could be indicative of a long-term deterioration of MKPCs in contact with neutral and basic environments that might be encountered when using these cements. This paper also discussed the appropriate drying method for studying MKPCs, since the drying method may change the microstructure and the properties of the materials which might lead to potentially misleading interpretations.

2. Experimental

2.1. Materials

The raw materials used in this study were hard-burnt magnesia (MgO: MAGCHEM 10 CR from M.A.F. Magnesite BV, having particle size distribution: d_{10} = 4.8 µm, d_{50} = 18.9 µm, d_{90} = 45.6 µm; specific surface area ≈ 0.9 m²/g; purity 98.3%; loss on ignition 0.25%); potassium dihydrogen phosphate KH_2PO_4 (VWR, purity > 98%, d_{10} = 175 µm, d_{50} = 365 µm, d_{90} = 594 µm), low-CaO content coal fly ash (d_{10} = 3.0 µm, d_{50} = 24.2 µm, d_{90} = 136.1 µm; specific surface area≈ 2.2 m²/g; composition given in Table 1), boric acid (H_3BO_3, VWR, purity 99.5%) and deionized water.

Table 1: Fly ash chemical composition (X-ray fluorescence)

Oxide	SiO_2	Al_2O_3	CaO	Fe_2O_3	MgO	K_2O	TiO_2	SO_3	Na_2O	P_2O_5	SrO	MnO
% (mass)	50.30	25.75	6.58	5.92	2.15	1.53	1.36	0.80	0.78	0.67	0.27	0.08

The cement paste was prepared with an Mg/P molar ratio kept to 1 and a water-to-cement weight ratio fixed at 0.56, slightly higher than the chemical demand of the cement for water (w/c = 0.51). The fly ash/cement (cement = MgO + KH_2PO_4) weight ratio was fixed at 1 in order to obtain good rheological properties. Boric acid was used as a setting retarder, at a boric-acid-to-cement weight ratio of 1.5%. The mixture proportions are presented in Table 2.

Table 2: Composition of magnesium phosphate cement pastes (2 liters MPC grouts were cast).

	MKPC	**Weight percentage**
Materials	**Weight (Kg/m^3)**	**%**
MgO	128.07	8.9
KH_2PO_4	432.24	29.9
Fly ash	560.21	38.8
Boric acid (H_3BO_3)	8.42	0.6
water	315.93	21.8

Small cylindrical and rectangular samples were cast in plastic boxes and kept sealed for 28 days (endogenous conditions with very low air content). Then some samples were kept in the boxes for 6 months and the others were divided into three groups:

- 1/ small cast monolithic samples were placed in 500 mL of four different solutions for 1 and 6 months for the characterization of the pore solution (MKPC-1M), porosity (MKPC-6M) and SEM observations (MKPC-6M).
- 2/ crushed powders (3 g) obtained from 28-day-old MKPC samples were placed in 30 mL solutions for 3 months (MKPC-3M). The crushed powders were used to optimize the contact surface area between solid and water in order to extrapolate mineralogical phenomena occurring in the long term in bulk samples (PXRD + quantitative Rietveld analyses, TGA analyses).

The composition of the four solutions is given in Table 3 and Table 4 summarizes names of the different samples studied in this paper.

Table 3: Composition of the four cementitious solutions placed in contact with MPC pastes for 1500 g of water.

Solution	pH	NaOH	KOH	$Ca(OH)_2$	Na_2CO_3	NaCl
Deionized water	6.8	-	-	-	-	-
Carbonated Water	10.9	-	-	-	0.72 g	-
Pore solution of CEM V*	13.2	3.99 g	11.22 g	0.11 g	-	-
Pore solution of CEM V* with chloride ions	13.3	3.99 g	11.22 g	0.11 g	-	3.55 g

* Simplified pore solutions of CEM V deprived of trace elements were used.

Table 4: Denomination of the samples studied in this paper

Categories		Name of samples		
Aging	**28 days**	MKPC-28D		
	1.5 months	MKPC-1M		
	3 months	MKPC-3M		
	6 months	MKPC-6M		
Solution	**Deionized water**	MKPC-1.5M_6.8	MKPC-3M_6.8	MKPC-6M_6.8
	Carbonated Water	MKPC-1.5M_10.9	MKPC-3M_10.9	MKPC-6M_10.9
	Pore solution of CEM V*	MKPC-1.5M_13.2	MKPC-3M_13.2	MKPC-6M_13.2
	Pore solution of CEM V* with chloride ions	MKPC-1.5M_13.3	MKPC-3M_13.3	MKPC-6M_13.3
Drying method	**without drying**	MKPC-28D		
	air (7 days)	MKPC-air		
	vacuum (2 days)	MKPC-vacuum		
	40°C (24 h)	MKPC-40		
	50°C (3 days)	MKPC-50		
	60°C (24 h)	MKPC-60		
	80°C (24 h)	MKPC-80		
	105°C (24 h)	MKPC-105		
	Freeze-drying (3 min in liquid nitrogen + 7 days)	MKPC-FD		

* Simplified pore solutions of CEM V deprived of trace elements were used.

2.2. Characterizations

Microstructural changes due to aging were investigated by following the changes is the mineral composition, pore solution and porosity. The MKPC pastes were primarily characterized after 28 days (MKPC-28D) of aging in endogenous conditions (sealed plastic boxes), and then characterized after 1, 3 and 6 months (MKPC-1M, MKPC-3M, MKPC-6M respectively) of aging in the 4 solutions: water, carbonated water, or pore solution of CEM V with or without NaCl (Table 3). MKPC paste was also

characterized after 6 months (MKPC-6M) of aging in endogenous conditions in order to gain a better understanding of the microstructural changes over time and to determine the effect of the 4 solutions on MKPC paste.

2.2.1 Solid characterizations

Several experimental techniques were used to characterize MKPC pastes. The solid phases were ground and rinsed with isopropanol, then dried and preserved in a partial vacuum using a desiccator. Crystallized phases were studied by powder X-ray diffraction (PXRD) using the PanAlytical X'pert Pro diffractometer equipped with X'celerator detector and having copper radiation ($\lambda K_{\alpha 1,2}$ = 1.54184 Å [Cu]) in the Bragg Brentano geometry. All the PXRD patterns of pastes ground by hand to a particle size less than 100 µm were collected in the range of 2θ = 5° to 100°, with 0.0167° steps for a total acquisition time of 2 hours. Qualitative analyses of the X-ray powder patterns were performed to identify crystalline phases, and mineral quantitative analyses were extracted from Rietveld treatments using the FullProf software [48]. The following six compounds were considered during Rietveld refinements: K-struvite ($KMgPO_4 \cdot 6H_2O$, *Pmn*2_1, *a* = 6.892 Å, *b* = 6.166 Å, *c* = 11.139 Å, 17 independant atomic positions including hydrogen [49]); mullite ($Al_{4.5}Si_{1.5}O_{9.75}$, *Pbam*, *a* = 7.58 Å, *b* = 7.68 Å, *c* = 2.98 Å, 6 independant atomic positions including one with static distribution between Al and Si [50]), quartz-alpha (SiO_2, *P*$3_2$21, *a* = 4.921 Å, *c* = 5.400 Å, 2 independant atomic positions [51]), MgO (*Fm*-3*m*, *a* = 4.214 Å, 2 independant atomic positions [52]), and KNO_3 (aragonite-type, *Pnma*, *a* = 6.436 Å, *b* = 5.530 Å, *c* = 9.192 Å, 4 independant atomic positions [53]). Quantitative results considering crystalline phases only were extracted directly from Rietveld analyses, and the presence of an amorphous contribution was estimated by considering the sum of mullite+quartz as the internal standard. The two mullite and quartz phases, considered as unreactive during the hydratation process and aging, came from the fly ash filler. In a first step, quantitative Rietveld analysis was performed on a fly ash sample containing 20.0 weight percent (wt %) of silicon as the internal standard, and determined the following composition: 11.8 wt % of mullite, 4.5 wt % of quartz and 83.7 wt % of glassy phase. Thus, the internal standard (mullite+quartz) for MKPC binder samples could be calculated at 6.5 wt %, allowing the quantitative analyses to be performed taking the presence of the amorphous part into account.

Thermogravimetric analyses (TGA) were carried out under argon atmosphere on 1 ± 0.1 g of a sample ground to about 80 µm using a NETZSCH STA 449F3 instrument at 10 °C / min up to 1000 °C.

Scanning electron microscopy (SEM) observations used a JEOL JSM-7800 F Prime scanning electron microscope and were carried out on freshly broken pieces (after carbon metallization). An analysis by electron probe micro analysis (EPMA) quantified each element in the volume analyzed as a percentage by weight of oxides. The equipment used was a CAMECA SX Five (Centre de Micro Caractérisation Raimond Castaing CMCR – UMS 3623) with an accelerating voltage of 10 kV and a current of 10 nA. The volume probed during each analysis was 2x2x2 μm^3. The following elements were analyzed: Mg, K, P, S, Cl, Ca, Si, Na and Fe (10s/element + 5s for the continuous background). These analyses used polished sections of MKPC pastes. Polishing was performed dry using silicon carbide discs. The polished sections were then covered with a carbon film for electronic conduction. Fracture sections on freshly broken pieces were also studied (SEM & EPMA).

^{31}P solid state NMR experiments were performed using a 300 MHz Bruker spectrometer at 121.49 MHz Larmor frequency. The experiments were carried out using magic angle spinning (MAS) at 10 kHz and a 4 mm-diameter zirconia rotor. ^{31}P MAS spectra were recorded using one pulse sequence with a recycling time of 50 s, and chemical shifts were calibrated using H_3PO_4 at 0 ppm.

2.2.2 Porosity characterizations

To obtain information on the size of the pores in the porous network, the mercury intrusion porosimetry (MIP) technique was used. The principle of this technique is to force the mercury into the sample by applying increasing pressure. The higher the pressure is, the more the mercury fills the small pores. If the pores are assumed to be cylindrical, pore radius is inversely proportional to the applied pressure [54, 55, 56]. The apparatus used for this study was a 140 Pascal coupled with 240 Pascal (Fusion Instrument) and the samples analyzed were about 1 cm^3 dried pieces that represented 3 g of MKPC pastes.

The porosity of MKPC pastes could not be measured by the nitrogen adsorption method (BJH method [57]), since K-struvite could not withstand the pressure of a high vacuum pump over a long time (40 hours).

2.2.3 Pore solution characterizations

A high-pressure device for extracting fluid from porous materials was used to obtain the pore solution of the MKPC pastes [58]. At various times, rectangular or cylindrical MPC paste samples were removed from their curing conditions and crushed to obtain pieces of around 20 mm. The apparatus used was composed of two thick cylinders, fitted into each other and standing on a base plate that contained the solution collector. The crushed sample (≈ 200 g) was then placed in the device and compressed by an axial load generated by a 3000 kN hydraulic press on a set of pistons. As the porous material was compressed, pore fluid was forced into a circular channel and then passed through one of the three holes drilled in the solution collector. The solution was collected in a small polypropylene recipient, which could be removed through a drawer system. The extraction was carried out on a 3000 kN Amsler compression testing machine, using a loading rate of 3 kN/s up to 1500 kN.

Directly after the extraction, the pH of the solution was measured using a standard pH meter (HACH PH31) previously calibrated between pH 6 and 10, and 10 and 13. Then the composition of the solution was analyzed by inductively coupled plasma optical emission spectroscopy (ICP-OES) and ion chromatography (IC).

The concentrations of Mg^{2+}, K^{+}, Na^{+}, Fe^{2+}/Fe^{3+}, Si^{4+}, Al^{3+}, Ca^{2+}, and borate ions were measured by ICP-OES using an Optima™ 7000 DV ICP-OES (PerkinElmer) equipped with a CCD sensor. Each analysis composition was filtered at 0.45 mm and subjected to an acid dilution of 2% in pure nitric acid. Finally, the results obtained were processed using WinLab32 treatment and acquisition software.

The concentrations of PO_4^{3-}, SO_4^{2-}, and Cl^{-} ions were measured using a Dionex ICS-39 with an AS-15 column and AG-15 precolumn. Thirty-eight (38) mmol/L of KOH was used as eluent at 30°C.

3. Results

3.1. Aging of MKPC pastes in endogenous conditions (cast in sealed plastic boxes)

The mineralogy, porosity and pore solution composition were determined for 28 day and 6 month old MKPC samples (MKPC-28D, MKPC-6M) kept in endogenous conditions (i.e. sealed plastic boxes).

3.1.1 Mineralogical evolutions

The phase assemblages of 28 day and 6 month old dried samples (MKPC-28D, MKPC-6M, refer to section 2.1.1 for the drying method) were characterized by PXRD (Figure 1) and thermogravimetric analyses (Figure 2). The crystallized phases were quantified by Rietveld analysis with an internal standard (Table 5).

After 28 days (MKPC-28D) and 6 months (MKPC-6M) of aging, PXRD patterns exhibited the same crystallized phases. K-struvite [$MgKPO_4.6H_2O$] was the main crystalline phase that precipitated during the MKPC hydration. Three minor phases were also identified: 1/ unreacted magnesium phosphate [MgO] (about 1 wt.% out of the 11 wt.% of MgO initially introduced in MKPC paste, Table 2), 2/ mullite [$3Al_2O_3.SiO_2$] and quartz [SiO_2] resulting from the fly ash addition (5 wt.% and 2 wt.%, respectively). Rietveld quantification highlighted an amorphous part in the samples, composed of the vitreous phase from fly ashes and a supplementary amorphous phase resulting from the MKPC hydration process. Table 5 shows that some of the K-struvite was not detected since the amount measured was different from that calculated (fly ash was assumed to be nonreactive as the pore solution pH value was close to neutrality). It should be borne in mind that pore solution (residual water + ions) should be considered to include this supplementary amorphous phase. The amorphous phase was observed to evolve over time from 17 wt.% for 28 day old samples (MKPC-28D) to 32 wt.% after 6 months of aging (MKPC-6M), the difference coming from the decrease in the crystalline K-struvite content (Table 5).

Thermogravimetric analyses confirmed the presence of K-struvite [$MgKPO_4.6H_2O$], known to have a dehydration temperature centered between 105 and 136 °C depending on the temperature rises [26, 59, 60] (≈ 136 °C for 10 °C/min). The two thermograms exhibited no change for K-struvite after 6 months of aging. The same weight loss of about 20 wt.% was observed, corresponding to 49 wt.% of K-struvite in samples (without considering the contribution of pore solution in Rietveld quantification). Coupling these results with the PXRD data indicating the increase of the proportion of amorphous part within the material, strongly suggested that some of the crystallized K-struvite was gradually transformed into a more amorphous phase by aging, without noteworthy modification of the chemical composition.

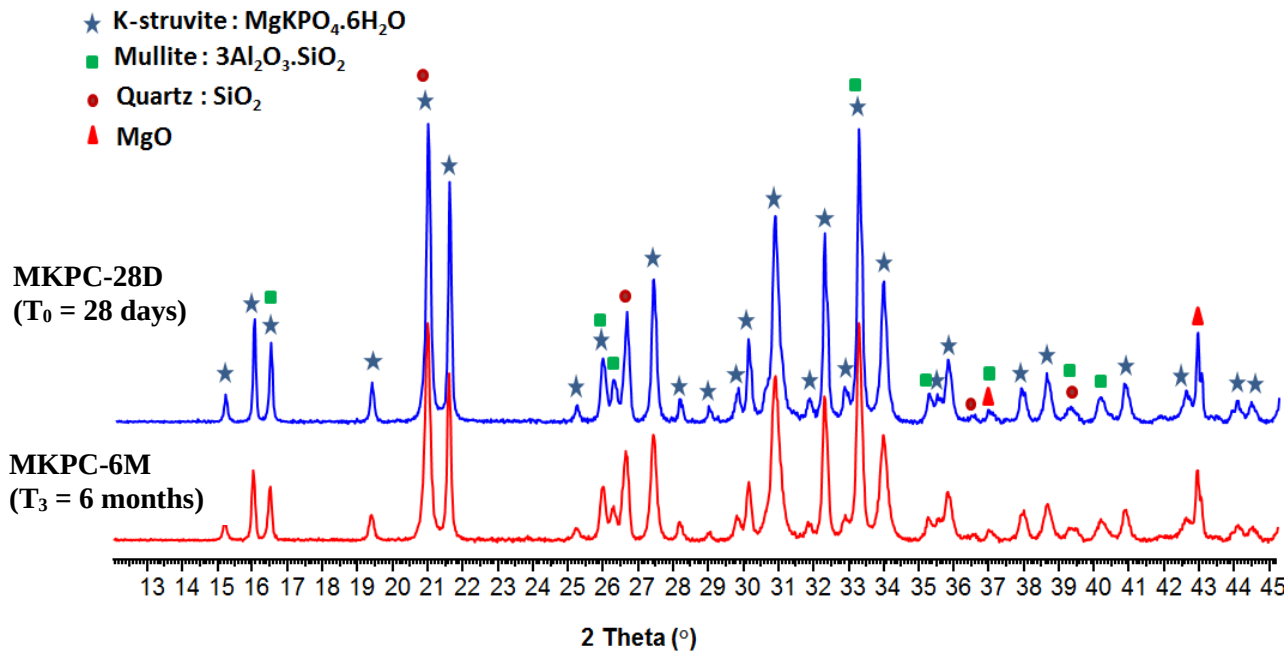

Figure 1: Diffractograms of 28 day old and 6 month old MKPC pastes (MKPC-28D, MKPC-6M) [MgO, KH_2PO_4, Fly ash, H_3BO_3, weight ratio w/c = 0.56, molar ratio Mg/P = 1].

Table 5: Mineralogical composition of 28 day old and 6 month old MKPC pastes (MKPC-28D, MKPC-6M) [MgO, KH_2PO_4, Fly ash, H_3BO_3, weight ratio w/c = 0.56, molar ratio Mg/P = 1]. Uncertainties are given in brackets.

Phases	MKPC-28D (wt.%) (28 days)		MKPC-6M (wt.%) (6 months)	
	Experimental value	Theoretical value	Experimental value	Theoretical value
$KMgPO_4.6H_2O$ (K-struvite)	42 ± 1	60.4	27 ± 1	60.4
$3Al_2O_3.SiO_2$ (mullite)	5 ± 1	4.7	5 ± 1	4.7
SiO_2 (quartz)	2 ± 1	1.8	2 ± 1	1.8
MgO (periclase)	1 ± 1	/	1 ± 1	/
Vitreous phase (Fly ash)**	33 ± 1	33.1	33 ± 1	33.1
Amorphous phase (difference)***	17 ± 5	/	32 ± 5	/

* Theoretical values were calculated by assuming all MgO and KH_2PO_4 participated in K-struvite precipitation.

** The amount of vitreous phase due to the presence of fly ash was calculated according to the mineralogical characterization of the raw material: 83.7 % for the vitreous phase, 11.8 % for the mullite and 4.5% for the quartz.

*** The amorphous phase was calculated by subtracting the contribution of the crystalline part and the fly ash from 100 wt%.

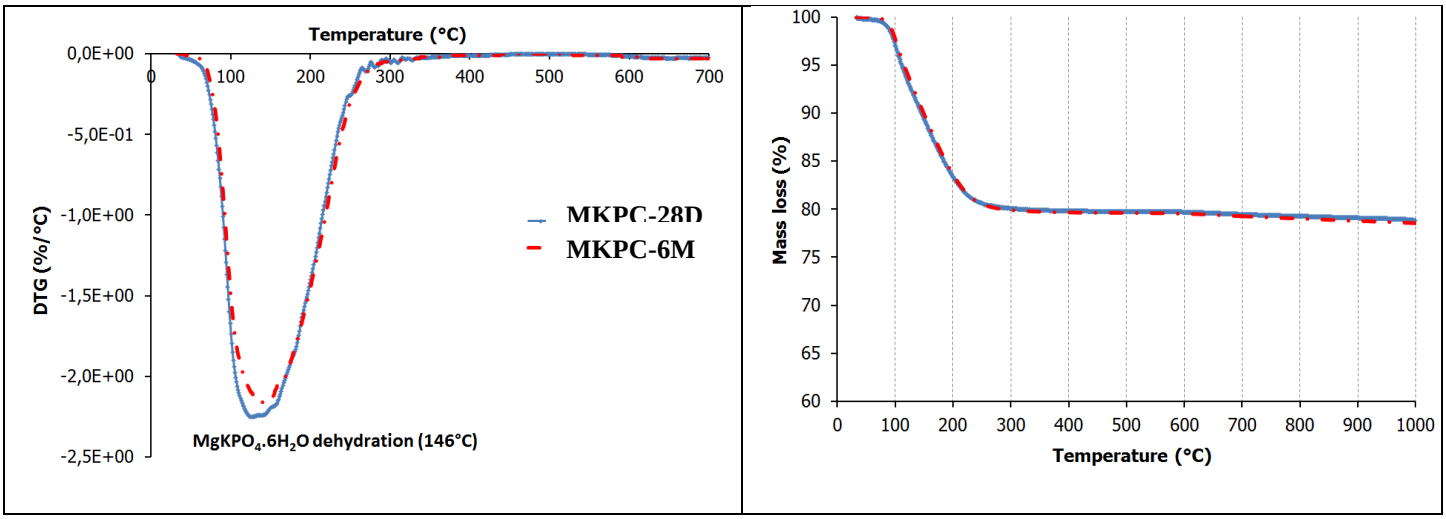

Figure 2: Thermogravimetric analyses of 28 day old and 6 month old MKPC pastes (MKPC-28D, MKPC-6M) [MgO, KH_2PO_4, Fly ash, H_3BO_3, weight ratio w/c = 0.56, molar ratio Mg/P = 1].

Polished and fractured sections of freshly broken pieces were analyzed by scanning electron microscopy (SEM) on a 6 month old sample of MKPC paste (MKPC-6M) kept in endogenous conditions. The SEM observations highlighted fly ash (spherical particles) surrounded by the MKPC cement paste. The pictures obtained on this sample showed that various morphologies could be observed for MKPC paste. Needles and tabular crystals were observed locally (Figure 3) as mentioned in previous papers [61, 62]. Figure 3 also shows that magnesium phosphate cement was sensitive to the drying method (high vacuum SEM), since cracks were observed in the cement paste as well as in K-struvite crystals [$MgKPO_4.6H_2O$]. EDX analyses gave the chemical composition of the cement paste and the fly ash.

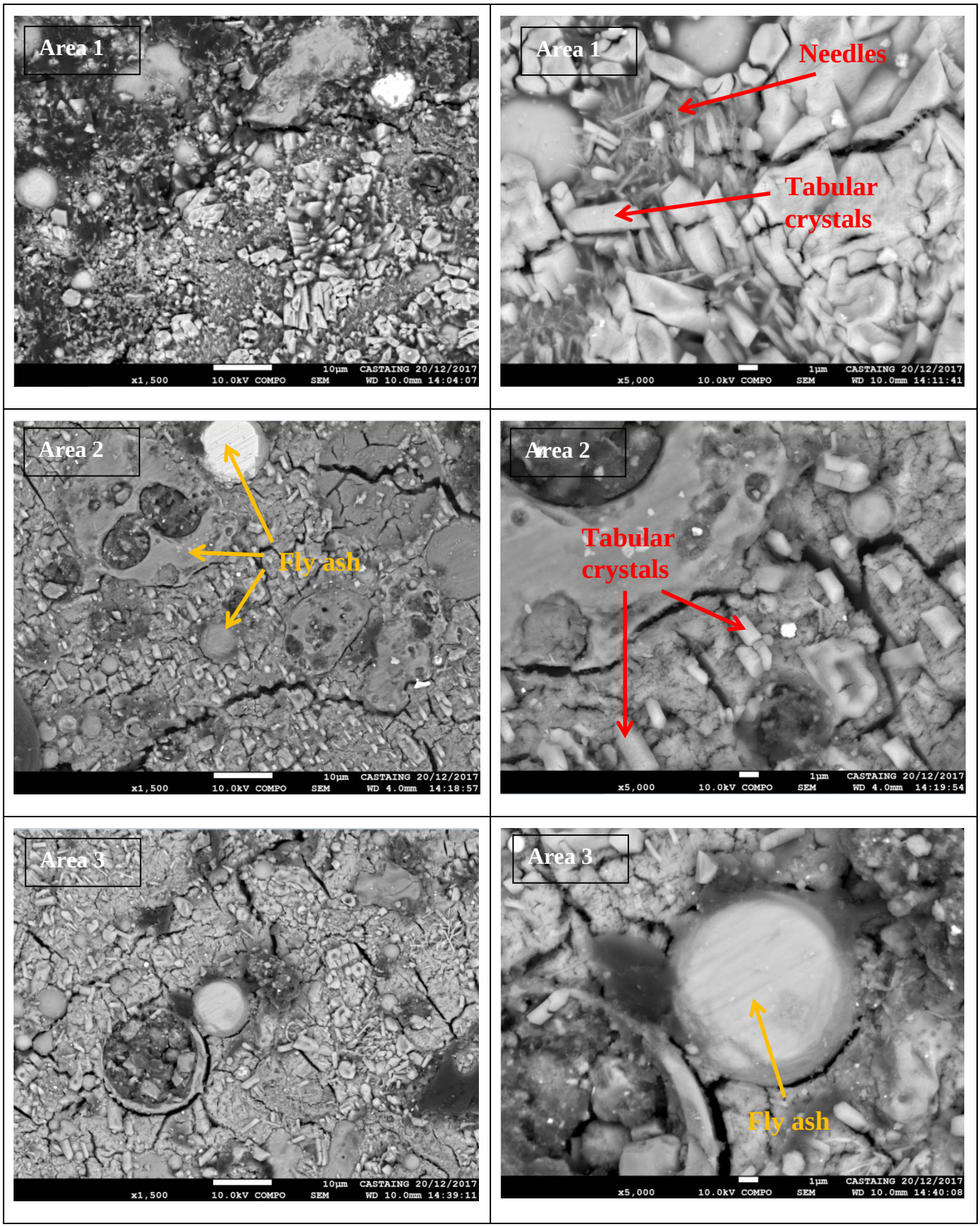

Figure 3: SEM observations of a 6 month old MKPC paste (MKPC-6M) kept in endogenous conditions for three areas and two magnification factors (x 1500 and x 5000) using backscattered electrons (polished sample).

Whatever the morphology analyzed (Figure 3), Mg/P, Mg/K and K/P molar ratios calculated from of EDX analyses were different from those characterizing stoichiometric K-struvite crystal [$MgKPO_4.6H_2O$, Mg/P = 1, Mg/K = 1, K/P = 1]. Mg/P, Mg/K and K/P molar ratios were between 0.62 and 0.94, 0.89 and 1.63, 0.55 and 0.92, respectively. Mg/K was the most sensitive ratio, with values below unity when zones with needle crystals were considered and above 1.4 when the continuous matrix was considered. This difference in morphology, combined with variation in chemical composition, could be correlated with the increasing rate of MKPC paste amorphization with time. Regarding the fly ash, a wide range of compositions were measured and aluminum (Al), silicon (Si), Iron (Fe) were the main elements detected. Mullite [$3Al_2O_3.SiO_2$] and quartz grain [SiO_2] could also be found.

3.1.2 Porosity features

The porosity of 28 day and 6 month old samples (MKPC-28D, MKPC-6M) was characterized by mercury intrusion porosimetry. It is reported in the literature that the porosity measured using mercury intrusion depends on the drying procedure of samples [42, 54, 55]. The influence of drying on MKPC pastes was therefore studied first.

3.1.2.1 Influence of the drying procedure applied to samples

Several drying methods were tested on small pieces of 28 day old MKPC pastes (± 2 to 3 cm samples, Table 4), and then the materials were characterized by PXRD with Rietveld analyses (Figure 4 and Table 6). The freeze-drying and high temperature drying methods (80 °C, 105 °C) proved to be unsuitable for MKPC paste drying: K-struvite crystals could not withstand such drying methods and so no crystalline K-struvite was detected by PXRD (MKPC-FD, MKPC-80, MKPC-105, Figure 4). Rietveld analyses highlighted a decrease of crystalline K-struvite when the temperature used for sample drying was increased, resulting in an increase of the amorphous phase: the 42 wt.% of crystalline K-struvite calculated in MKPC paste before drying became 37 wt.%, 26 wt.% or 0 wt.% after one night at 40 °C (MKPC-40), 60 °C (MKPC-60) or 80°C (MKPC-80), respectively. The least damaging method for drying MKPC pastes proved to be drying in a soft vacuum system (desiccator) after having immersed small samples in isopropanol for one week. According to Rietveld analysis, even drying at low

temperature, such as 40°C for 1 night or 50°C for 3 days (until constant weight), may damage K-struvite. (Table 6).

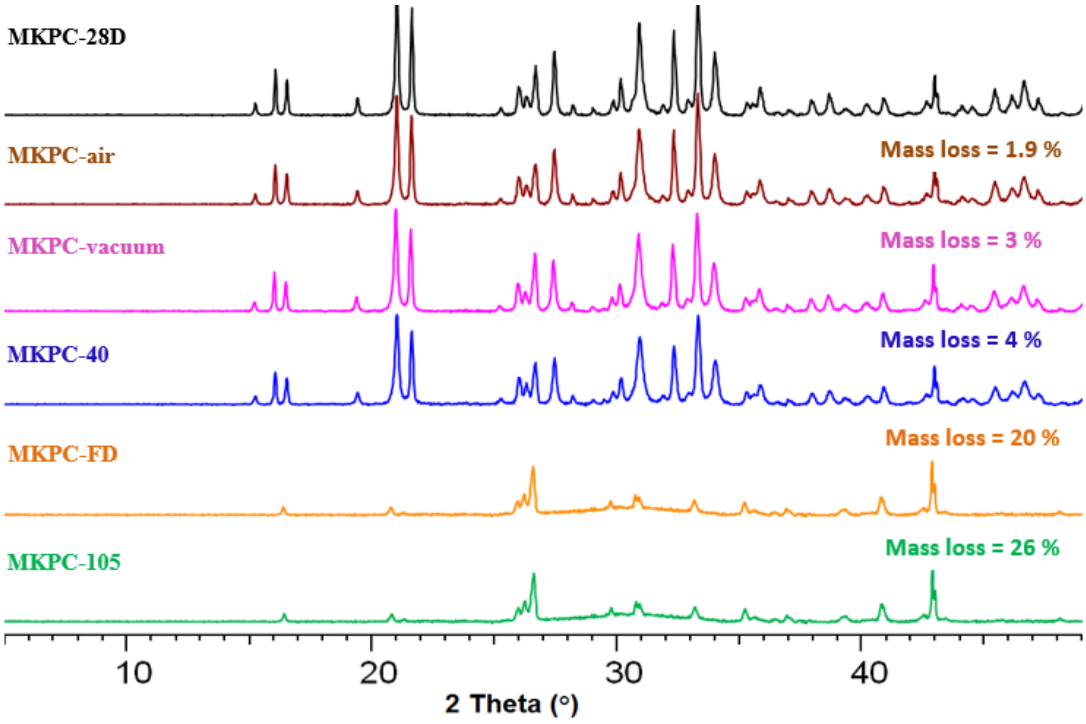

Figure 4: X-ray diffraction patterns of MKPC paste [MgO, KH_2PO_4, Fly ash, H_3BO_3, and H_2O, weight ratio w/c = 0.56, molar ratio Mg/P = 1] after several drying.

Table 6: Influence of the drying method on MKPC paste mineralogy.

Sample	Drying method	Mineralogical composition (wt.%)	Mineralogical composition evolution (wt.%)	K-struvite grain size(Å)
MKPC-28D	Without drying	K-struvite: 42 % Mullite: 5 % Quartz: 2 % MgO: 1 % Fly ash contribution: 33% Amorphous phase*: 17%	/	380
MKPC-vacuum	3 days in a partial vacuum (desiccator)	**Drying**: 3 %** K-struvite: 42 % Mullite: 5 % Quartz: 2 % MgO: 1 % Fly ash contribution: 33% Amorphous phase*: 14%	K-struvite: 0 % Amorphous phase*: -3 % **Drying**: 3 %**	365

MKPC-40	24 h at 40°C	**Drying**: 4 %** K-struvite: 37 % Mullite: 5 % Quartz: 2 % MgO: 1 % Fly ash contribution: 33% Amorphous phase*: 18%	K-struvite: -5 % Amorphous phase*: +1 % **Drying**: 4 %**	330
MKPC-50	3 days at 50°C	**Drying**: 6 %** K-struvite: 33 % Mullite: 5 % Quartz: 2 % MgO: 1 % Fly ash contribution: 33% Amorphous phase*: 20 %	K-struvite: -9 % Amorphous phase*: +3 % **Drying**: 6 %**	320
MKPC-60	24 h at 60°C	**Drying**: 8 %** K-struvite: 26 % Mullite: 5 % Quartz: 2 % MgO: 1 % Fly ash contribution: 33% Amorphous phase*: 25%	K-struvite: -16 % Amorphous phase*: +8 % **Drying**: 8 %**	300
MKPC-80	24 h at 80°C	**Drying**: 17 %** K-struvite : 0 % Mullite : 5 % Quartz : 2 % MgO : 1 % $Mg_2P_2O_7$: 1 % Fly ash contribution: 33% Amorphous phase*: 41%	K-struvite: -42 % Amorphous phase*: +24 % **Drying**: 17 %**	/
MKPC-105	24 h at 105°C	**Drying**: 26 %** K-struvite : 0 % Mullite : 5 % Quartz : 2 % MgO : 1 % $Mg_2P_2O_7$: 1 % Fly ash contribution: 33% Amorphous phase*: 32%	K-struvite: -42 % Amorphous phase*: +15 % **Drying**: 26 %**	/
MKPC-FD	Freeze-drying method (3 min in liquid nitrogen + 7 days in freeze-dryer)	**Drying**: 20 %** K-struvite : 0 % Mullite : 5 % Quartz : 2 % MgO : 1 % $Mg_2P_2O_7$: 1 % Fly ash contribution: 33% Amorphous phase*: 38%	K-struvite: -42 % Amorphous phase*: +21 % **Drying**: 20 %**	/

* The amorphous phase was calculated as the difference between 100 % and the contribution of the crystalline part + fly ash.

** Drying = mass of water lost.

Mercury intrusion porosimetry tests on 28 day old MKPC samples (MKPC-28D) showed a total pore volume of 14.2% for samples dried in a desiccator for 3 days (MKPC-vacuum) and 19.8 % for samples dried at 50 °C for 3 days (MKPC-50). The pore size distributions were also quite different (Figure 5). After 3 days of drying at 50°C, the small pores (10 nm to 100 nm in diameter) in MKPC pastes had disappeared and larger pores were observed. For this reason, it was decided to use the partial vacuum drying method (desiccator) for characterizing the porosity of MKPC pastes by mercury intrusion porosimetry in this study.

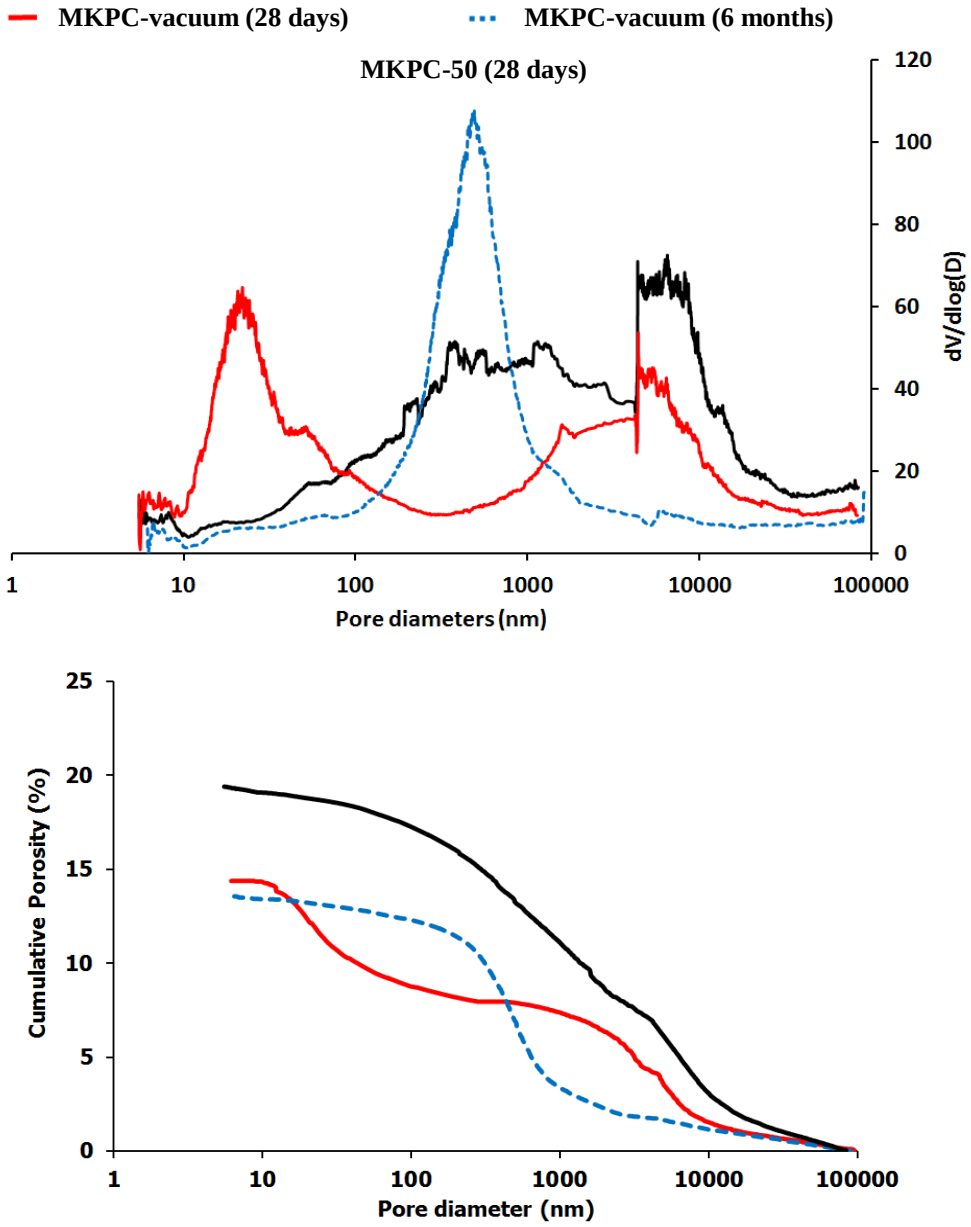

Figure 5: Pore size distribution (diameters) and cumulative porosity of 28 day and 6 month old MKPC pastes (MKCP-28D, MKPC-6M) [MgO, KH_2PO_4, Fly ash, H_3BO_3, weight ratio w/c = 0.56, molar ratio Mg/P = 1]. Two drying methods are compared for 28 old day samples: 3 days of drying in a desiccator (MKPC-vacuum) or at 50 °C (MKPC-50).

3.1.2.2 Porosity evolution with aging

The porosity of 28 day old and 6 month old MKPC paste samples (MKPC-28D, MKPC-6M) preserved in endogenous conditions and dried in a desiccator were measured by mercury intrusion porosimetry (refer to section 2.1.1 for the drying method). Any differences observed were small. Total pore volumes equal to 14.2 % and 13.6 % were measured for the 28 day old and 6 month old samples, respectively. However, the pore size distributions obtained were quite different, the 28 day old sample (MKPC-28D) presented a bimodal distribution (20 nm and 5000 nm centered families; Figure 5), while a practically monomodal pore size distribution (or more precisely a tightened bimodal distribution between 100 nm and 1000 nm diameter) was measured for the 6 month old sample (MKPC-6M, Figure 5). A smaller critical pore diameter was measured for the 6 month old sample (an evolution from 10000 nm to 1000 nm of the critical pore diameter was observed with aging). This observation could be explained by the filling of large pores and might be related to the amorphization of the material.

3.1.3 Evolution of the pore solution with aging

The pore solutions of 28 day and 6 month old samples kept in endogenous conditions were extracted (MKPC-28D, MKPC-6M). The composition of these two pore solutions is given in Table 7. Changes observed in ion concentrations ($[PO_4^{3-}]$, $[K^+]$, $[B^{3+}]$, $[Mg^{2+}]$) were consistent with an evolution of the material over time, as hydration was still in progress. The decrease in $[PO_4^{3-}]$, $[K^+]$, $[B^{3+}]$, $[Mg^{2+}]$ might be consistent with the precipitation of additional K-struvite type phases and borate compounds.

Table 7: The pH and composition of the pore solution of MKPC paste at 28 days and 6 months [MgO, KH_2PO_4, Fly ash, H_3BO_3, weight ratio w/c = 0.56, molar ratio Mg/P = 1]. DL: Detection Limit (it can't be measured).

	MKPC-28D 28 days	MKPC-6M 6 months
	7.8 < pH < 9	8.1 < pH < 9
Chemical species	Concentration (mmol/L)	Concentration (mmol/L)
PO_4^{3-}	648	445
SO_4^{2-}	158	139
Cl^-	< DL	< DL
$B^{(3+)}$	186	87
K^+	1419	1108
Mg^{2+}	7	3.9
Na^+	25	8.7
Ca^{2+}	1.2	0.8
Si^{4+}	4.8	2.8

3.2. Aging of MKPC pastes in neutral and basic solutions

Rectangular and cylindrical samples were kept for 6 months in 4 different solutions (Table 3, Table 4). Crushed powders were also placed in contact with these solutions for 3 months to accelerate exchanges between liquid and solid; i.e. to speed up the potential mineralogical modifications and to provide a better understanding of physicochemical processes that might be involved in extended exposure conditions.

3.2.1 Influence of aging on MKPC pastes mineralogy

3.2.1.1 Considering contact with crushed powders

After 3 months, the crushed powders immersed in the four solutions were recovered (MKPC-3M_6.8, MKPC-3M_10.9, MKPC-3M_13.2, MKPC-3M_13.3, Table 4), filtered under isopropanol and dried in a partial vacuum (desiccator). Then the crushed powders were characterized by PXRD and Thermogravimetric analyses. Crystalline phases were quantified by Rietveld analysis.

Diffractograms showed some mineralogical shifts depending on the solution in contact with the MKPC pastes (Figure 6). As regards MKPC pastes in contact with deionized water (pH = 6.8) and carbonated water (pH = 10.9), no new crystalline phase was detected (MKPC-3M_6.8, MKPC-3M_10.9). However,

diffraction peaks of K-struvite [$MgKPO_4.6H_2O$] were observed to be narrower than the reference, indicating an evolution toward better crystallinity of K-struvite in deionized and carbonated waters (pH values lower than 11). The big crystals having a morphology looking like the well-known K-struvite crystals [61, 62] on SEM observations could explain this observation (Figure 11). In contrast, for MKPC pastes in contact with basic solutions with or without chloride ions (pH = 13.3), bumps on the diffractograms for small angles indicated the presence of a new, poorly crystalline phase (MKPC-3M_13.2, MKPC-3M_13.3). Apart from these observations, in basic solutions, the widths of K-struvite peaks were preserved and variation on the relative peak intensities was also noted (see the two diffraction peaks close to 2 theta = 16° for example). Rietveld processing enabled these evolutions in relative intensities to be explained by means of a preferential orientation model, indicating that, unlike crystal morphology (platy (or tabular) or needle-shaped crystals lead to preferential orientation on X-ray powder patterns), the crystallinity of K-struvite did not progress on contact with alkaline solution.

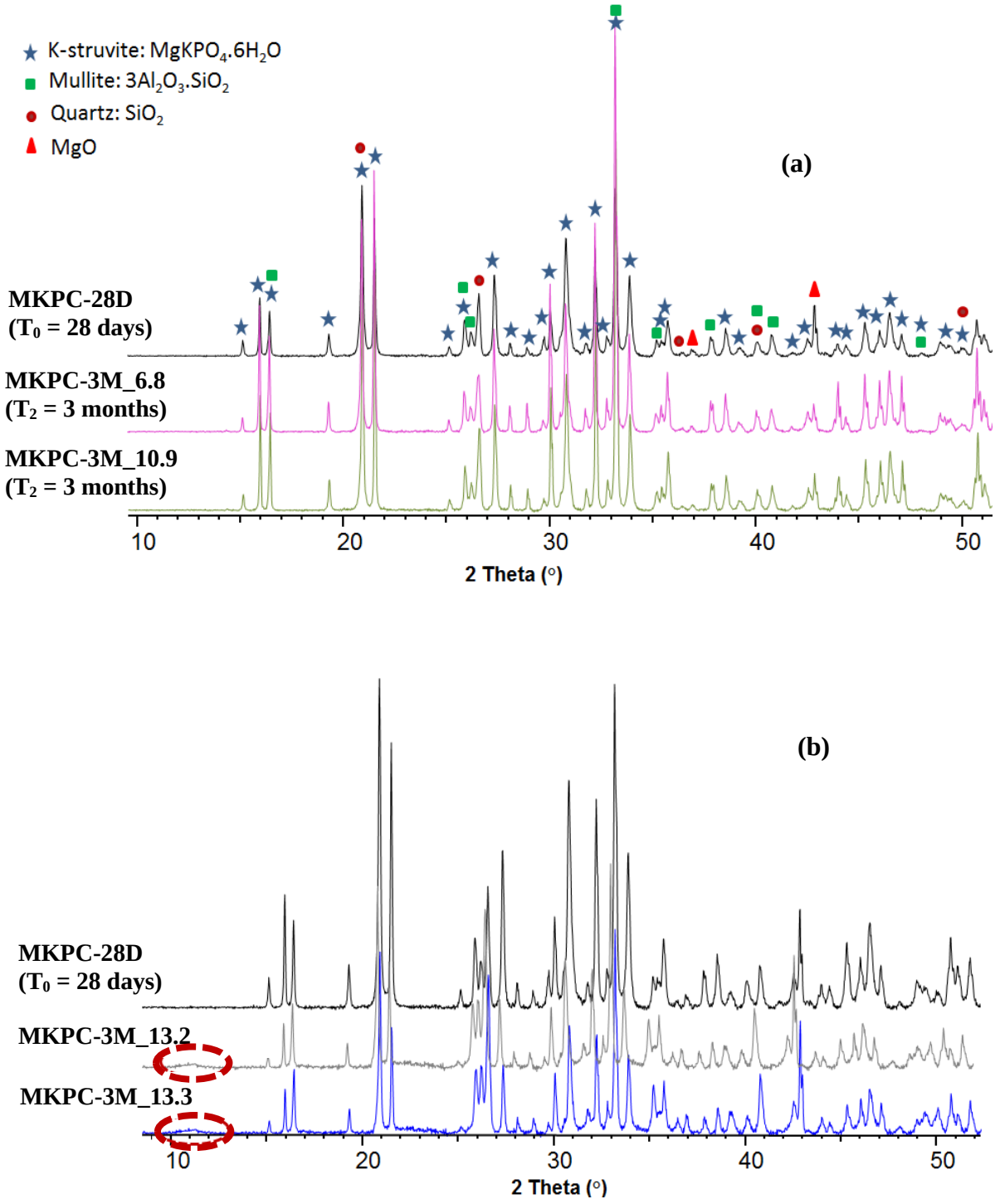

Figure 6: Diffractograms of crushed powders immersed in deionized water and carbonated water for 3 months (a), and in CEM V pore solution with or without chloride ions for 3 months (b) [MgO, KH_2PO_4, Fly ash, H_3BO_3, weight ratio w/c = 0.56, molar ratio Mg/P = 1].

Moreover, Rietveld quantification revealed a decrease in the amount of crystalline K-struvite whatever the solutions used, implying an increase in the calculated amorphous phase content. This decrease of crystalline struvite content, which seems to be more marked in basic solutions during the first months of interaction, was interpreted by the amorphization of the MKPC pastes. Table 8 shows that amorphization observed on crushed MKPC powder immersed in deionized water (pH = 6.8) or carbonated water (10.9) was of the same order of magnitude as the amorphization previously observed for natural aging of MKPC pastes (6 months in endogenous conditions). Unlike water immersion, the contact of crushed MKPC powder with alkaline solutions significantly increased the rate of amorphization of K-struvite. Similar observations were made after 6 months of contact (MKPC-6M), showing the conservation of the amorphization rate in water solutions (similar to that in endogenous conditions), and the increase of amorphization rate in alkaline conditions (Figure 7: amorphization rate was calculated by the ratio of amorphous phase wt.% to the theoretical K-struvite wt.%).

Table 8: Mineralogical composition of MKPC pastes preserved in different conditions: samples kept in endogeneous conditions for 28 days and 6 months and the crushed powders being immersed for 3 months in the 4 solutions (Table 3). Uncertainties are given in brackets.

Phases (wt. %)	MKPC-28D No contact	MKPC-6M No contact	MKPC-3M_6.8 (D. Water)	MKPC-3M_10.9 (Carb. Water)	MKPC-3M_13.2 (CEM V)	MKPC-3M_13.3 (CEM V+ NaCl)
K-struvite	42 ± 1	27 ± 1	28 ± 1	29 ± 1	14 ± 1	12 ± 1
Mullite	5 ± 1	5 ± 1	5 ± 1	5 ± 1	5 ± 1	5 ± 1
Quartz	2 ± 1	2 ± 1	2 ± 1	2 ± 1	2 ± 1	2 ± 1
MgO	1 ± 1	1 ± 1	1 ± 1	1 ± 1	2 ± 1	1 ± 1
Vitreous phase (fly ash)	33 ± 1	33 ± 1	33 ± 1	33 ± 1	33 ± 1	33 ± 1
Amorphous phase* (difference)	17 ± 5	32 ± 5	31 ± 5	30 ± 5	44 ± 5	47 ± 5

* The amorphous phase is calculated as the difference between 100 % and the crystalline part + fly ash contribution.

3.2.1.2 Considering contact with bulk samples

The immersion of the rectangular or cylindrical bulk MKPC pastes in contact with the four different aqueous solutions was less penalizing. Since it took longer for the solutions to penetrate into the porosity of the material and for hydrates to form, a diffusion process took place and delayed the mineralogical

changes. The amorphization was still observed but increased slowly over time, similarly to endogenous aging. Figure 7, which displays the amorphization rate of K-struvite according the different environments, illustrates the fact that alkaline solutions interact more strongly. It is important to mention, however, that the differences observed in the bulk samples were not significant (contrary to crushed powders).

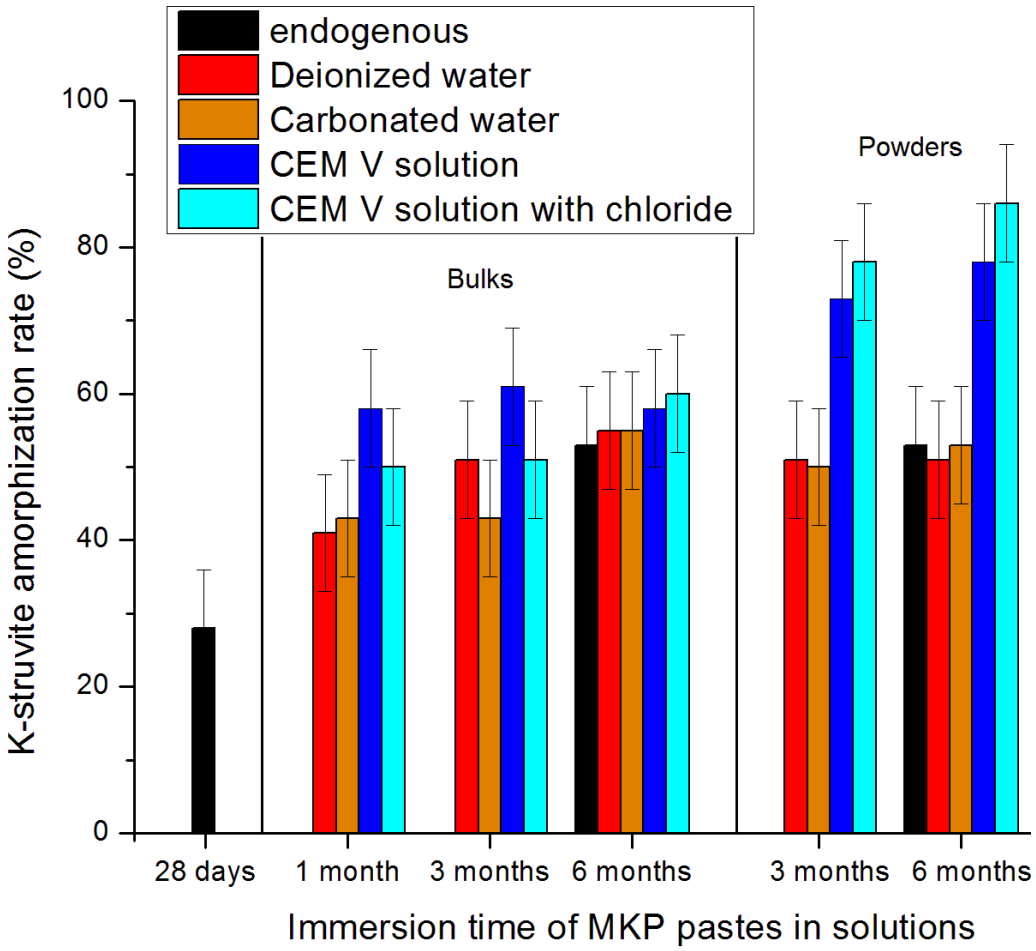

Figure 7: Evolution of the amorphization of K-struvite with time in MKPC pastes kept in different conditions (endogenous, deionized water, carbonated water, pore solution of CEM V with or without chloride ions). Uncertainties were calculated considering the uncertainty on the calculated amorphous phase and the theoretical amount of K-struvite that should have precipitated (Table 5).

3.2.1.3 Thermogravimetric analyses

The thermograms obtained on crushed powders immersed for 3 months give additional information (Figure 8). Regarding the crushed powders immersed in deionized or carbonated waters for 3 months (pH values lower than 11, MKPC-3M_6.8, MKPC-3M_10.9), a larger amount of bound water was

detected in MKPC pastes. Their weight loss of 22 to 23%, corresponding to 56 wt.% of K-struvite [$MgKPO_4.6H_2O$], matches the sum of crystalline K-struvite + amorphous phase determined by PXRD analyses (i.e. about 59 wt.%). Despite the loss of crystallinity according to X-Ray powder diffraction, K-struvite [$MgKPO_4.6H_2O$] stayed stable in these solutions (as shown by the equivalent DTG plots centered around 136 °C). This indicates that the amount of K-struvite not detectable by PXRD corresponds only to a loss of crystallinity (loss of long-range order by the introduction of numerous structural faults: stacking faults, substitution, hydration, carbonation, etc.) and not to a real destabilization of the mineral species. Regarding the crushed powders immersed in alkaline solutions for 3 months (pH values around 13.3, MKPC-3M_13.2, MKPC-3M_13.3), a smaller amount of bound water was detected in MKPC pastes. DTG plots shifted towards lower temperature and a supplementary weight loss was also observed at higher temperature, around 350 °C (Figure 8-b). These TGA results, combined with PXRD analyses, highlight a more complex behavior in alkaline solution. In addition to the crystalline and amorphous K-struvite phases (total amount about 30 wt.%), an effective K-struvite destabilization that should be correlated with the observed new poorly crystallized phase must be considered. The broad diffraction peak at low angles and the decomposition around 350 °C [63, 64] may suggest a brucite-like lamellar compound; an LDH type compound known to be stable in alkaline solutions.

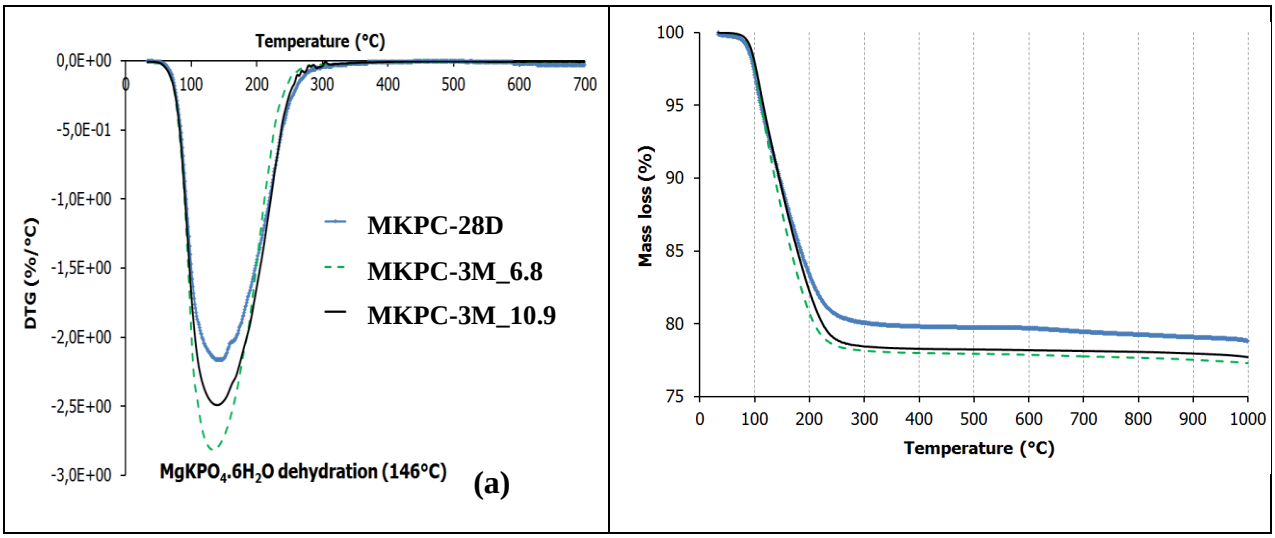

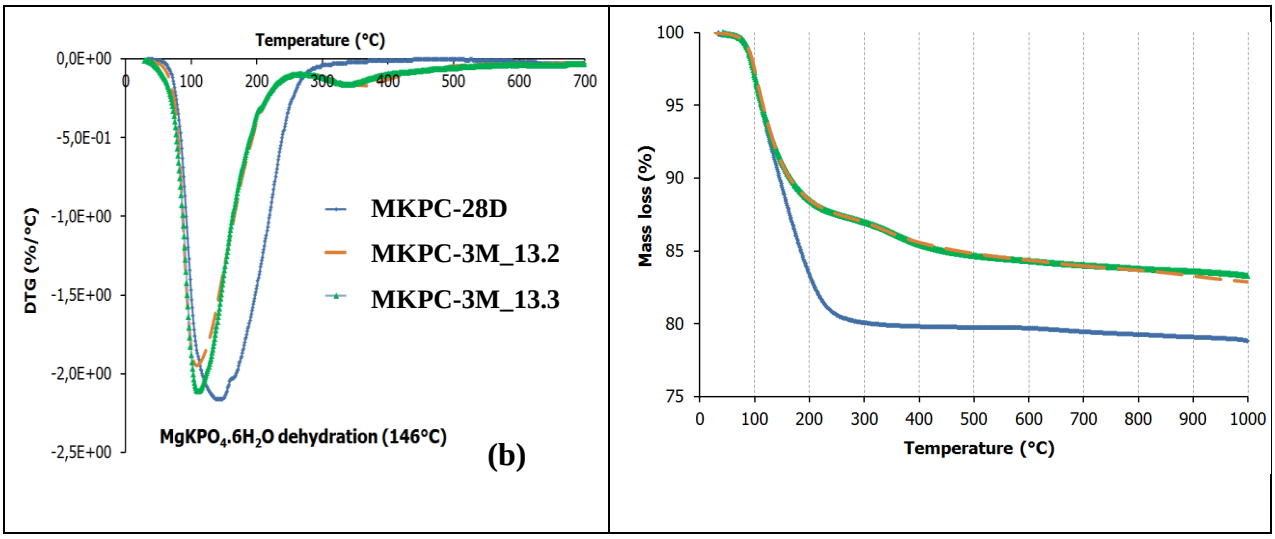

Figure 8: Thermogravimetric analyses of crushed powders immersed for 3 months in deionized water and carbonated water (a), pore solution CEM V with or without chloride ions (b) [MgO, KH_2PO_4, Fly ash, H_3BO_3, weight ratio w/c = 0.56, molar ratio Mg/P = 1].

3.2.1.4 SEM observations

Lastly, SEM observations were also carried out on two 6 month old samples of MKPC paste kept in deionized water (MKPC-6M_6.8) and pore solution of CEM V containing chloride ions (MKPC-6M_13.3), and compared with SEM observations on the 6 month old sample of MKPC paste kept in endogenous conditions (MKPC-6M, Figure 4). The two main phases – fly ash and the cement paste – were still easily differentiable in the material. Regarding the sample kept for 6 months in the alkaline solution (CEM V + NaCl, pH = 13.3), only a continuous morphology was observed for the cement paste throughout the material. The tabular or needle crystals observed on the 6 month old sample kept in endogenous conditions were no longer observed (Figure 9). However, crystals containing sodium were observed on fracture observations (Figure 10). EDX chemical analyses from these large newly precipitated crystals are given in Table 9. It might be Hazenite ($Mg_2KNa(PO_4)_2.14H_2O$), an analogous phase of K-struvite ($MgKPO_4.6H_2O$) that could not be identified easily by X-ray powder pattern as its crystal structure corresponds to a superstructure (ordered Na - K substitution) [65]. Furthermore, its dehydration temperature (183°C) [66] is close to the dehydration temperature of K-struvite (136 °C) [26].

Regarding the sample kept in the neutral solution (deionized water, pH = 6.8) for 6 months, a continuous morphology was also observed (Figure 11). However big crystals having a morphology looking like the

well-known K-struvite crystals [61, 62] were also present throughout the material. These observations could explain the better crystallinity of K-struvite (Figure 6-a, narrower diffraction peaks of K-struvite) together with an amorphization process (corresponding to the continuous morphology). The calculated molar ratios (Mg/P, Mg/K and K/P) deviated from the ideal K-struvite composition [$MgKPO_4.6H_2O$, Mg/P = 1, Mg/K = 1, K/P = 1] for both continuous and crystallized zones as already observed. Nevertheless, in presence of sodium, the Mg/P, Mg/(K+Na) and (K+Na)/P ratios were very close to unity. It is thus difficult to interpret these two antagonistic observations: one part of K-struvite loses in crystallinity while another part gains. The presence of impurities, which can substitute for elements of K-struvite in a more or less ordered way, might explain these observations. In addition, the differences from unity for the Mg/P, Mg/K and K/P ratios can be explained by the presence of potassium to proton substitution (H^+ not detectable by EDX), corresponding to the pH-dependent PO_4^{3-} to HPO_4^{2-} substitution.

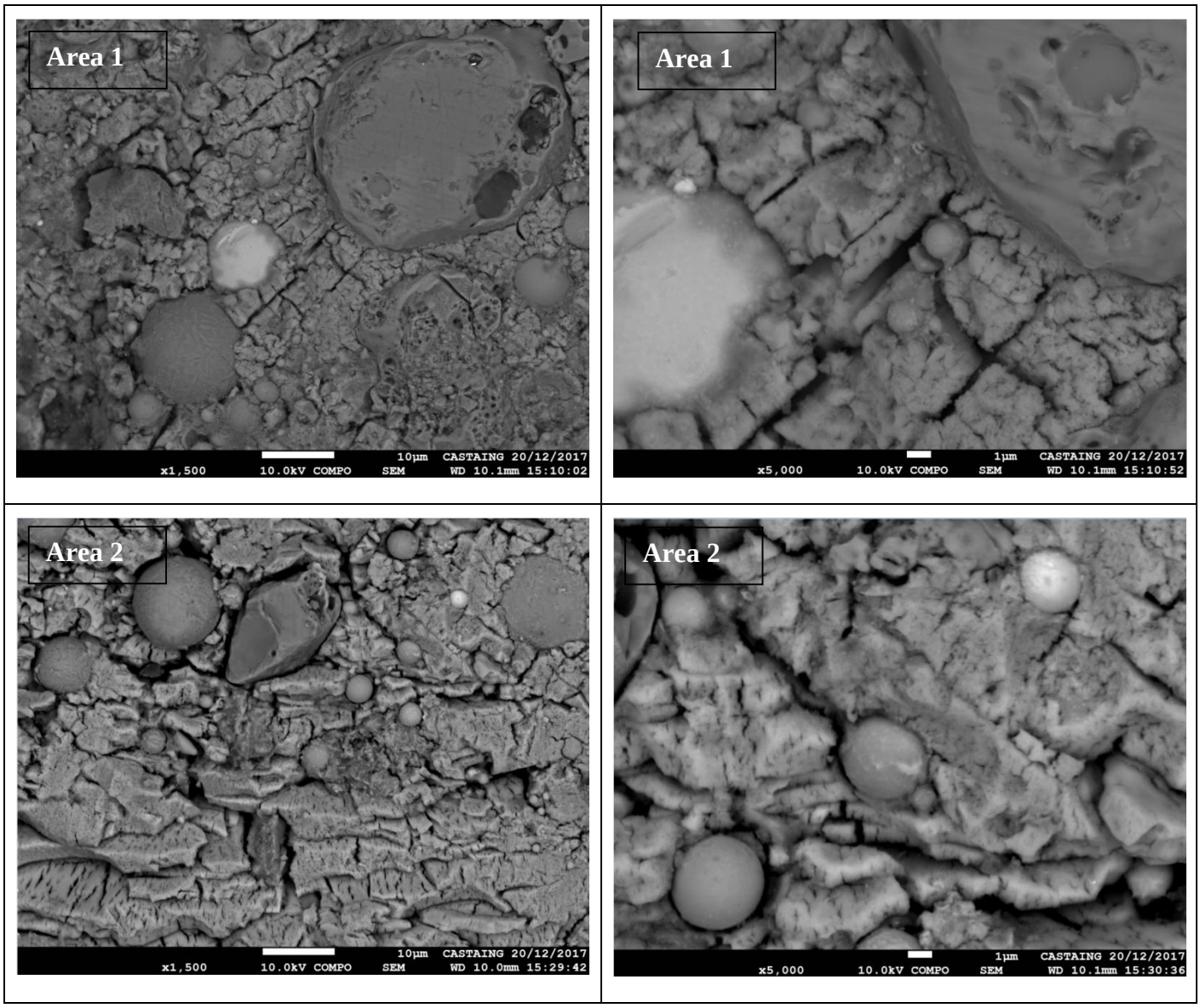

Figure 9: SEM observations of a 6 month old MKPC paste kept in CEM V pore solution with chloride ions for two areas and two magnification factors (x 1500 and x 5000) using backscattered electrons (polished sample, MKPC-6M_13.3).

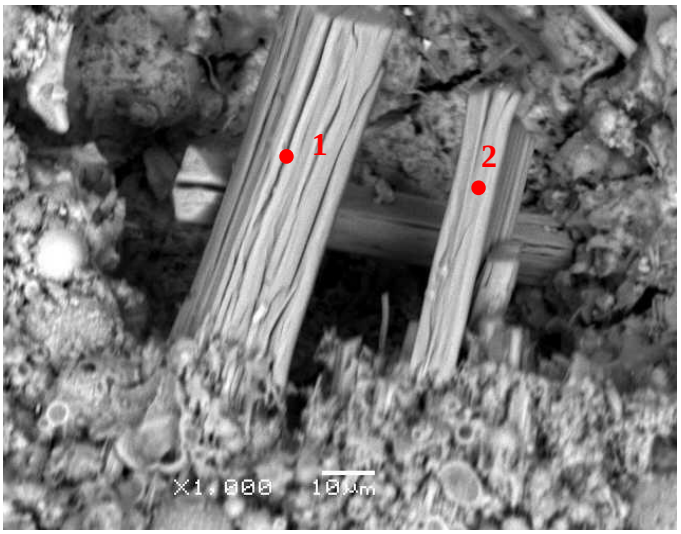

Figure 10: SEM observation of a 6 month old MKPC paste kept in CEM V pore solution containing chloride ions (MKPC-6M_13.3) using backscattered electrons (fracture sample).

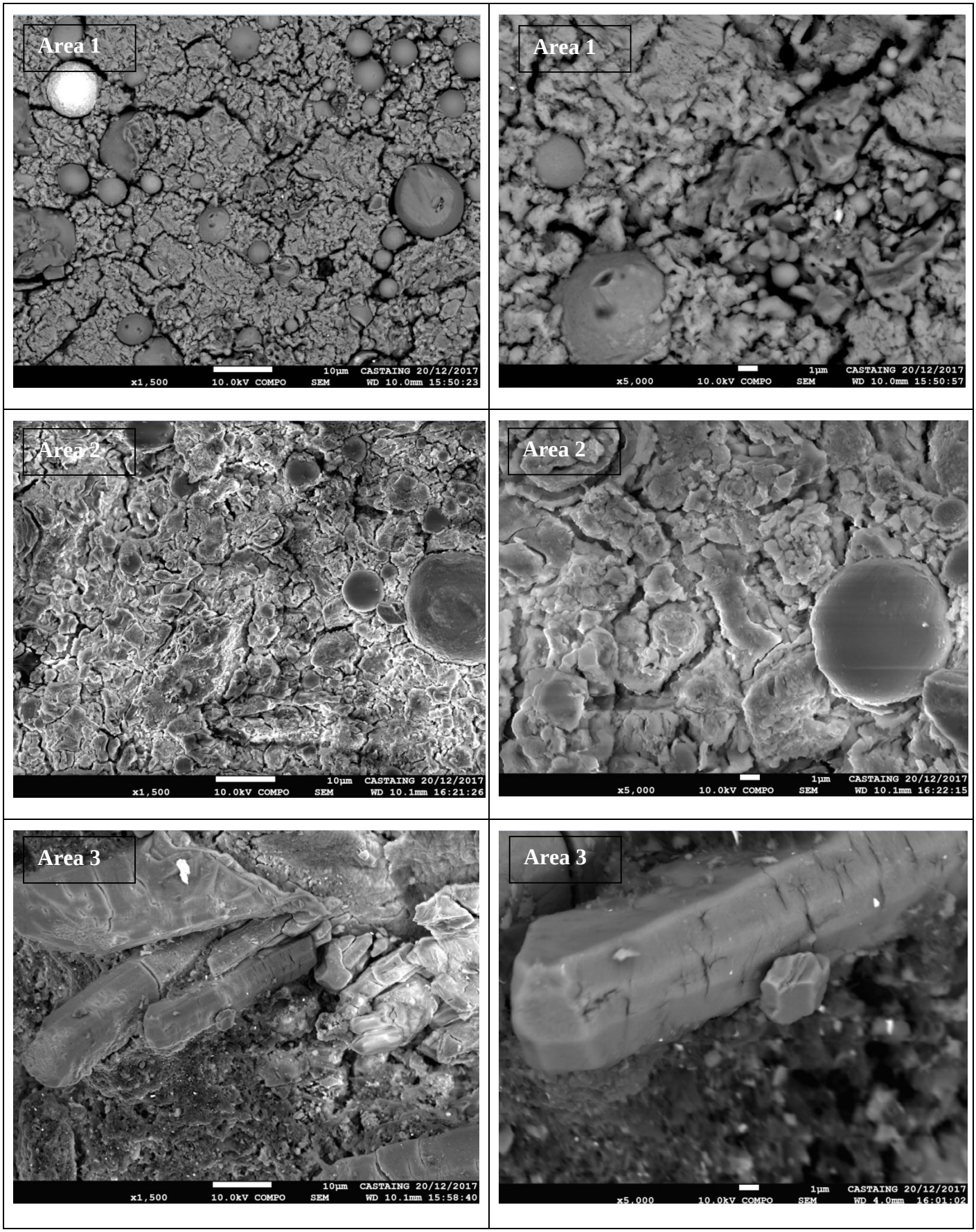

Figure 11: SEM observations of a 6 month old MKPC paste kept in deionized water (MKPC-6M_6.8), for three areas and two magnification factors (x 1500 and x 5000) using backscattered electrons (polished sample).

Table 9: Elemental composition (%wt.) of crystals observed within MKPC paste kept in a basic solution (Figure 10) and related molar ratios Mg/P, Mg/K and K/P calculated from EDX analyses (MKPC-6M_13.3).

	Chemical elements (% wt.)					Molar ratios		
Spectra	**O**	**Mg**	**P**	**K**	**Na**	**Mg/P**	**Mg/(K+Na)**	**(K+Na)/P**
1	42.30	15.16	20.71	14.96	6.68	0.93	0.93	1.00
2	42.60	15.71	20.70	13.88	6.71	0.96	1.00	0.96

Finally, a mean elemental composition was calculated from 50 EDX analyses on fracture samples (continuous matrix). Some changes were observed in molar ratios Mg/P, Mg/K, K/P depending on the storage conditions (Figure 13). Mg/P ≈ 0.87, Mg/K ≈ 0.92, K/P ≈ 0.95 were calculated for the sample kept in endogenous conditions for 6 months (MKPC-6M), while Mg/P ≈ 1.64, Mg/(K+Na) ≈ 1.40, (K+Na)/P ≈ 1.17, Na/K ≈ 0.29 and Mg/P ≈ 0.91, Mg/K ≈ 1.08, K/P ≈ 0.84 were calculated for the sample kept for 6 months in pore solution of CEM V containing chloride ions and in deionized water (MKPC-6M_13.3, MKPC-6M_6.8), respectively. These calculations showed that the non-stoichiometry in K-struvite depends on storage conditions; i.e. is due to a multiple substitution mechanism. A substitution of potassium ions (K^+) by sodium ions (Na^+) was clearly evidenced for the sample kept in the basic solution in particular. Excess of magnesium was detected punctually in this cement paste, which could be explained by the presence of an additional brucite-like phase stable in alkaline mediums.

3.2.2 Influence of aging on porosity of MKPC pastes

The porosities of MKPC paste samples immersed for 6 months in neutral and basic solutions (MKPC-6M_6.8, MKPC-6M_10.9, MKPC-6M_13.2, MKPC-6M_13.3) were measured by mercury intrusion porosimetry and then compared to the porosities of 28 day old and 6 month old samples kept in endogenous conditions (MKPC-28D, MKPC-6M, Figure 12). In all cases, the results showed a change with respect to the initial pore size distribution. No change in total volume porosity (14.4 %) was observed for the samples immersed for 6 months in deionized water (about the same total pore volume as measured for samples kept in endogenous conditions), unlike the situation in other immersion solutions. The total porosity increased slightly in carbonated water (17.1 %) and considerably in alkaline

solutions (23.1% and 23.7 % measured for samples immersed in CEM V with and without chloride ions, respectively). The increase in porosity volume is assumed to be related to the apparition of a mesopore size family (pore diameter below 100 nm; Figure 12).

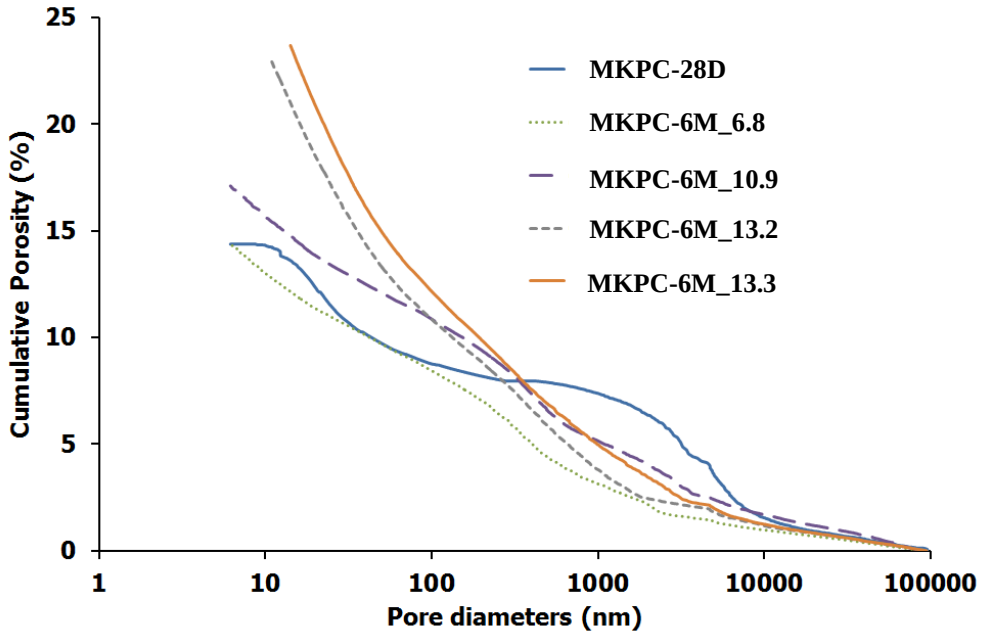

Figure 12: Pore size distribution (diameters) and cumulative porosity of 28 day old and 6 month old MKPC paste immersed in deionized water, carbonated water, pore solution of CEM with or without chloride [MgO, KH_2PO_4, fly ash, H_3BO_3, weight ratio w/c = 0.56, molar ratio Mg/P = 1].

3.2.3 Influence of aging on MKPC paste pore solution

To obtain a better understanding of the physicochemical processes that might be involved, the pore solutions of MKPC pastes were extracted after being in contact with the 4 solutions for 1.5 months (Table 3). The pore solutions were extracted from 10 cylindrical samples (about 200 g) kept in the cementitious solutions (500 mL) by applying a pressure of 530 MPa (1500 kN). The surfaces of these samples were dried with paper before the pore solution was extracted. Then, the pH value and the composition of the pore solutions of MKPC pastes were measured and compared to those extracted from 28 day old samples kept in endogenous conditions (MKPC-28D). Table 10 shows the pH and composition evolutions of the four extracted pore solutions.

Pore solutions of MKPC pastes (MKPC-1.5M_10.9, MKPC-1.5M_6.8) immersed in carbonated water (pH = 10.9) and deionized water (pH = 6.8) presented pH values similar to that of pore solution extracted from endogenous MKPC paste (pH ≈ 8.5, Table 10). However, some changes in ion concentrations were observed:

- leaching of the initial pore solution (28 day old MKPC pastes) was observed, with a significant decrease of the following concentrations: $[PO_4^{3-}]$, $[SO_4^{2-}]$, $[B^{3+}]$, $[K^+]$ (a mean dilution factor of 7.2),

Pore solutions of MKPC pastes (MKPC-1.5M_13.2, MKPC-1.5M_13.3) immersed in pore solution of CEM V with and without chloride ions (pH ≈ 13.3) for 1.5 months exhibited a pH increased to alkaline values (11-12, Table 10). This evolution is evidence of the penetration of the simulated cementitious solution into the MKPC paste porosity, thus implying expected chemical interactions. It could be noted that:

- leaching of the initial pore solution (28 day old MKPC pastes) was still observed, although to a smaller extent, except for sulfate anions (mean dilution factors equal to 4.5 for $[PO_4^{3-}]$, $[B^{3+}]$, $[K^+]$ and 15 for $[SO_4^{2-}]$). The global decrease of the dilution effect is easily explained by the fact that the contact solution was initially charged in ionic species, and the sharp disappearance of sulfate anions should be due to calcium sulfate precipitation.

- penetration of chloride and sodium ions within the material was also observed. When present, such ions are known to cause durability problems (pitting corrosion on metals [67] and alkali-aggregate reaction [68, 69]).

Table 10: Evolution of the pH and the composition of the pore solution of MKPC paste after 1.5 months' contact with carbonated water (pH = 10.9) and deionized water (pH = 6.8) [MgO, KH_2PO_4, Fly ash, H_3BO_3, weight ratio w/c = 0.56, molar ratio Mg/P = 1]. DL: Detection Limit (it can't be measured); tr: traces (measured in very low concentration)

	MKPC-28D	MKPC-1.5M_13.3 (CEM V + NaCl)	MKPC-1.5M_13.2 (CEM V)	MKPC-1.5M_10.9 (Carb. Water)	MKPC-1.5M_6.8 (D. Water)
	7.8 < pH < 9	pH = 11.8	pH = 11.2	pH = 8.6	pH = 8.5
Chemical species	**Concentration (mmol/L)**	**Concentration (mmol/L)**	**Concentration (mmol/L)**	**Concentration (mmol/L)**	**Concentration (mmol/L)**
PO_4^{3-}	648	131	130	76	70
SO_4^{2-}	158	10	11	16	14
Cl^-	< DL	32	< DL	< DL	< DL
$B^{(3+)}$	186	42	47	28	24
K^+	1419	318	335	188	170
Mg^{2+}	7	< DL	< DL	1.2	1.7
Na^+	25	116	80	4,9	< DL
Ca^{2+}	1,2	tr	tr	< DL	< DL
Si^{4+}	4.8	1	1.2	0.8	1.1

4. Discussion of the durability of MPC pastes over time and in contact with neutral and basic solutions

4.1 What is amorphization of MKPC pastes?

Our results showed that an amorphization process of MKPC pastes was observed over time. The different morphologies observed (needle crystals and continuous matrix, Figure 3), combined with the variation in chemical composition could be correlated with the increasing rate of MKPC paste amorphization with time.

The amorphization rate was maintained in case of contact with neutral aqueous solution and was accentuated for contact with cementitious basic solutions (with or without chloride ions at pH ≈ 13.3) according to XRD analyses and quantitative Rietveld analyses carried out on crushed powder samples. When bulk materials were considered, the natural amorphization of MKPC pastes was still observed, but was no longer dependent on the storage conditions (an equivalent amorphization rate was determined for all the bulk samples after 6 months of aging, Figure 7).

Thermogravimetric analyses and SEM observations revealed some structural changes in the K-struvite phase over time (Figure 2 and Figure 3). For example, molar ratios of Mg/P ≈ 0.87, Mg/K ≈ 0.92, K/P ≈ 0.95 were calculated for the sample kept in endogenous conditions for 6 months (MKPC-6M). Thus, the ideal K-struvite $MgKPO_4.6H_2O$ (Mg/P = 1, Mg/K = 1, K/P = 1) could have turned out to be $Mg_{0.87}K_{0.95}(PO_4)_{0.69}(HPO_4)_{0.31}.6H_2O$ after 6 months of aging in endogenous conditions, taking the balance of charges into account. These structural changes, implying a cationic deficient structure and a PO_4^{3-}/HPO_4^{2-} statistical disorder (Figure 14), could explain the observed loss of crystalline phase (actually a less crystallized, disordered K-struvite phase). The disorder created could be seen either by proton to potassium and magnesium substitution, or by a hydrogeno-phosphate to phosphate substitution (which should be pH dependent).

As regards the samples immersed for 6 months in deionized water (MKPC-6M_6.8) and in pore solution of CEM V containing chloride ions (MKPC-6M_13.3), Mg/P ≈ 0.91, Mg/K ≈ 1.08, K/P ≈ 0.84 (deionized water) and Mg/P ≈ 1.64, Mg/(K+Na) ≈ 1.40, (K+Na)/P ≈ 1.17, Na/K ≈ 0.29 (CEM V) were calculated, respectively. In these cases, it might be more difficult to use the same logic, since thermogravimetric analyses on crushed powder showed that other phases could precipitate (Figure 8). In deionized water (MKPC-6M_6.8), a larger amount of bound water was detected in MKPC pastes (a mass loss of 23 % compared with 20% for samples kept in endogenous conditions), poorly crystallized K-struvite could precipitate and $Mg_{0.91}K_{0.84}(PO_4)_{0.66}(HPO_4)_{0.34}.(6+0.9)H_2O$ would represent the cement paste according to the molar ratios calculated taking the balance of charges into account. In the pore solution of CEM V containing chloride ions (MKPC-6M_13.3), the possible presence of a lamellar brucite-based compound is evidenced by the extremely large Mg/P and Mg/(K+Na) ratios. The presence of two hydrates, combined with the sodium to potassium substitution in K-struvite (possibly leading to the ordered Hazenite ($Mg_2KNa(PO_4)_2.14H_2O$ compound, Figure 10) did not allow an averaged K-struvite composition to be calculated. Figure 13 clearly shows the single phase feature (when considering the hydrated cementitious matrix) for MKPC in contact with deionized water, which contrasts with the two-end feature for contact with CEMV containing chloride contacts. In the first case (Figure 13-a) all compositions determined are located around the theoretical K-struvite composition,

with the average composition not far away. For the second case (Figure 13-b) the compositions determined are organized along the segment between the (0,0) coordinate (corresponding to the lamellar brucite-based compound) and the (1,1) coordinate (corresponding to K-struvite). The last graph (Figure 13-c), expressing (K+Na)/Mg also shows a segment that illustrates the sodium to potassium substitution corresponding to the $MgK_{1-x}Na_x(PO_4)\cdot 6H_2O$ right end-member.

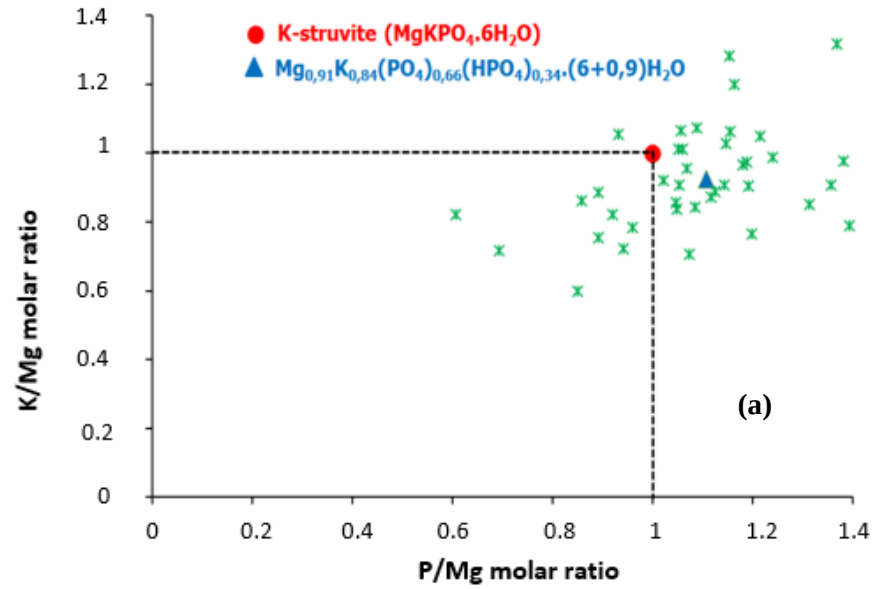

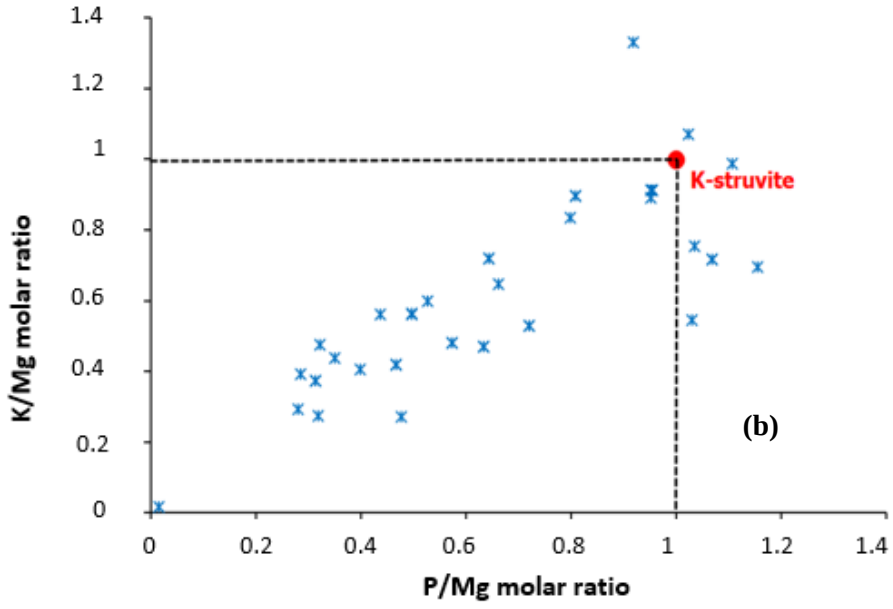

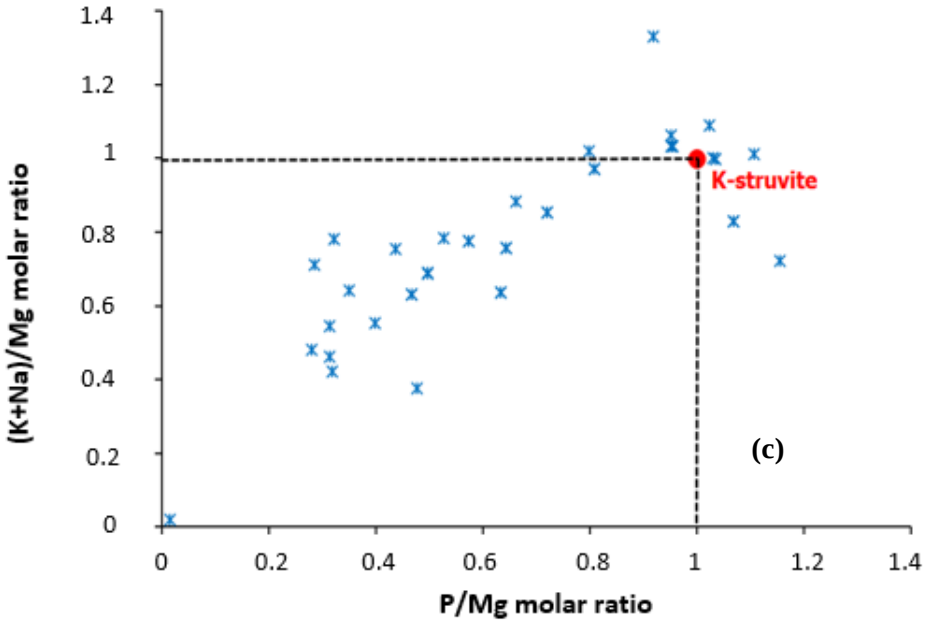

Figure 13: K/Mg or (K+Na)/Mg molar ratios vs P/M molar ratio of MKPC matrix for 3 samples (based on EDX analyses): sample kept 6 months in endogeneous conditions (MKPC-6M, (a)), sample kept 6 months in deionized water (MKPC-6M_6.8, (b)), sample kept 6 months in CEM V pore solution containing chloride ions (MKPC-6M_13.3) [MgO, KH_2PO_4, Fly ash, H_3BO_3, weight ratio w/c = 0.56, molar ratio Mg/P = 1].

Thus, the amorphization process of the material on aging, which is accentuated for crushed powders in contact with alkaline solutions, corresponds to a loss of crystallinity of the K-struvite structure due to proton substitution on the potassium site (leading, in fact, to a PO_4^{3-}/HPO_4^{2-} statistical disorder). In the case of alkaline contact, the formation of lamellar brucite-based hydrate explains the increase of the calculated amorphous content and sodium to potassium substitution also occurs. This result was confirmed by 31P MAS NMR spectroscopy, which evidenced the presence hydrogeno-phosphate anions in MKPC paste (Figure 14): the main signal at 6.6 ppm is attributed to (expected) PO_4^{3-} anions in K-struvite, and the well described shoulder at 3.0 ppm and 1.3 ppm is attributed to HPO_4^{2-} anion (according to NMR assignment of $Mg_2KH(PO_4)_2{\cdot}15H_2O$ [29], and $MgH(PO4){\cdot}7H_2O$ [29], respectively).

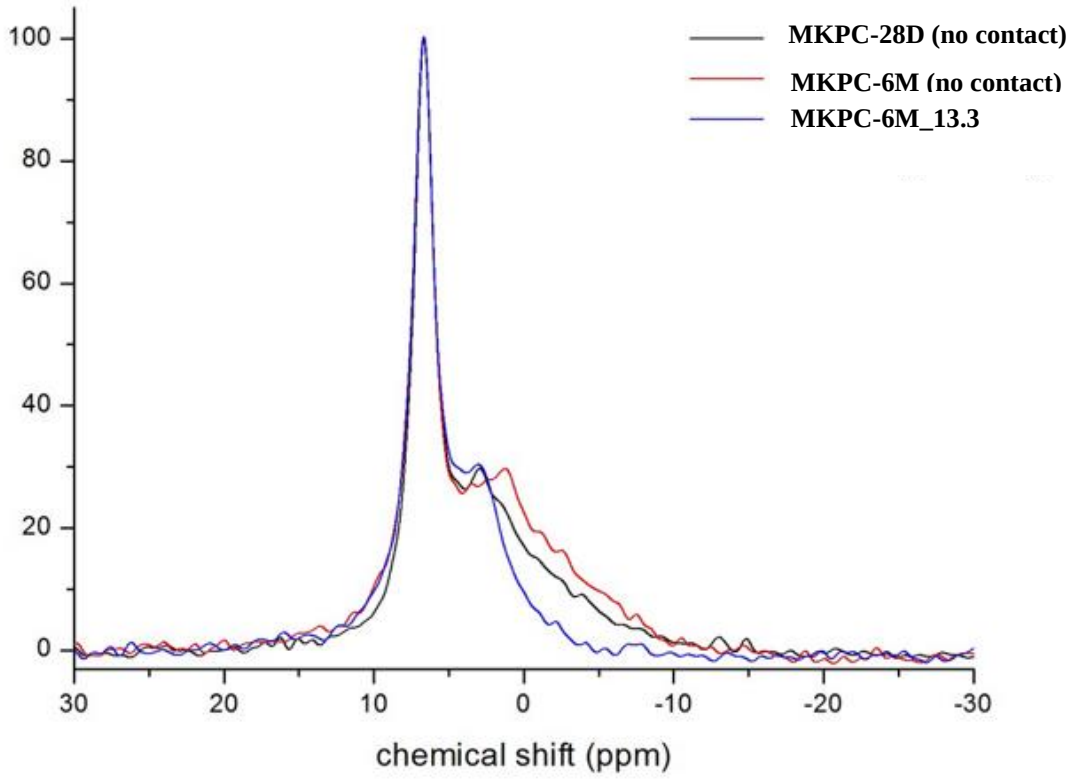

Figure 14: ^{31}P MAS NMR spectra of a 28 day old and 6 month old MKPC pastes kept in endogenous conditions (no contact) or in alkaline solution (pore solution of CEM V).

4.2 What is the durability of MKPC pastes over time in contact with neutral and alkaline solutions?

The study of the porosity of a material is very important to assess its durability, since it is directly linked to mechanical and transport properties.

The amorphization over time observed for the sample kept in endogenous conditions did not seem to influence the total porosity of the material. A total porosity of about 14 % was measured by mercury intrusion porosimetry for the 28 day and 6 month old samples (MKPC-28D, MKPC-6M, Figure 5).

However, porosity changes were observed for MKPC pastes kept in contact with different solutions. In all cases, the pore size distribution changed in comparison with the initial pore size distribution (Figure 12). Total porosities of 14.38 %, 17.11 %, 23.14 % and 23.70 % were measured for the samples

kept for 6 months in deionized water, carbonated water and pore solution of CEM V with or without chloride ions (MKPC-6M_6.8, MKPC-6M_10.9, MKPC-6M_13.2, MKPC-6M_13.3) respectively. Such evolutions in porosity would influence the transport and mechanical properties of the material, so higher open porosity and permeability, and changes in tortuosity could be expected. Furthermore, a loss of compressive strength could be observed as mentioned in the literature [39-41], especially in an alkaline medium.

Pore solution analyses of MKPC pastes kept for 1 month in deionized water (pH = 6.8) and carbonated water (pH = 10.9) exhibited similar pH values (pH ≈ 8.5), although the pore solution composition changed, with leaching of some elements of the initial pore solution (28 day old MKPC pastes) (Table 10). However, an increase of the pH up to about 12 was observed for samples kept in alkaline media (pore solution of CEM V with or without NaCl). This increase in pH could also have an impact on the stability of K-struvite and thus on the mechanical properties of the material. The PO_4^{3-} phosphate anion is stabilized by alkaline pH, but the presence of sodium leads to sodium - potassium substitution.

According to PHREEQC software and its thermodynamic database supplemented with aqueous boron-containing species and phosphate minerals [26, 70], K-struvite ($MgKPO_4.6H_2O \rightarrow Mg^{2+} + K^+ + PO_4^{3-} + 6H_2O$, pKs = 11 [71]) might be more soluble in basic media (Table 11). The calculations for 100 g of K-struvite in 1 liter solutions were in good agreement with TGA analysis, where less bound water was observed after the immersion of MKPC pastes for 6 months in the pore solution of CEM V with or without chloride ions (Figure 8-b, Table 11). Again according to PHREEQC software, bobierrite [$Mg_3(PO_4)_2.8H_2O$] and brucite-like $Mg(OH)_2$ might precipitate as a result of K-struvite dissolution (Table 10). Increases and decreases of pH were also observed depending on the solutions, the precipitation of brucite [$Mg(OH)_2$] yielding an increase of pH up to 11.2 for the deionized water and carbonated water. Nevertheless, even though there might have been dissolution of K-struvite in basic solutions, a significant volume of solution would be necessary to dissolve all the K-struvite hydrate. It would take about 4 liters of pore solution of CEM V to completely dissolve 100 g of K-struvite, diffusion processes being overlooked.

Table 11: Stability of K-struvite [$MgKPO_4.6H_2O$] in contact with the 4 solutions studied; calculations were made with PHREEQC software. Bound water measured with TGA analyses for 6 month old samples.

Solution (1 L)	K-struvite	$pH_{initial}$ (experiment)	pH_{final} (calculations)	Precipitated phases	Bound water (wt. %)
No contact	100	-	-	-	20
Deionized water	96.1	6.8	11.2	0.12 g $Mg(OH)_2$ 1.95 g $Mg_3(PO_4)_2.8H_2O$	23
Carbonated Water	95.8	10.9	11.2	0.14 g $Mg(OH)_2$ 2.06 g $Mg_3(PO_4)_2.8H_2O$	22
Pore solution of CEM V	74.4	13.2	12.1	5.83 g $Mg(OH)_2$	17
Pore solution of CEM V with chloride ions	74.4	13.3	12.1	5.83 g $Mg(OH)_2$	17

Thus, the immersion of MKPC paste in aqueous solutions (deionized water, carbonated water, and pore solution of CEM V with or without chloride ions) for a long time might lead to changes in the transport and mechanical properties of the material. In basic media, a loss of compressive strength and a higher permeability of the material are to be expected, since total porosity increases with the pH and some of the K-struvite might dissolve. The resistance of MKPC mortars to basic media seemed to be closely related to the stability of the hydration product $MgKPO_4.6H_2O$ (K-struvite).

5. Conclusion

Our work was aimed at understanding the microstructural behavior of MKPC paste over time in contact with neutral or basic solutions; media that MKPC paste might encounter when used as a patch repair material or as blocking material for hazardous wastes.

The study on ground powders and bulk samples gave an overview of the microstructure (PXRD-QPA, TGA, SEM-EDX) and the pore solution of MKPC pastes in different storage conditions: endogenous conditions [plastic boxes], deionized water [pH = 6.8], carbonated water [pH = 10.9], and pore solution of CEM V with or without chloride ions [pH ≈ 13.3]. This study highlighted an amorphization of MKPC paste over time, whatever the preservation conditions. This amorphization resulted from a smaller

amount of crystallized K-struvite [$MgKPO_4.6H_2O$] in the material. Stronger amorphization was observed in basic media (especially for ground powder in contact with the solutions). Structural changes of K-struvite [$MgKPO_4.6H_2O$] depending on the preservation conditions were considered to explain this amorphization, such as $Mg_{0.87}K_{0.95}(PO_4)_{0.69}(HPO_4)_{0.31}.6H_2O$ and $Mg_{0.91}K_{0.84}(PO_4)_{0.66}(HPO_4)_{0.34}.(6+0.9)H_2O$ after 6 months of immersion in endogenous conditions and deionized water, respectively. In basic solutions, a substitution of potassium ions by sodium ions (≈ 30 % in pore solution of CEM V) might take place.

The durability of MKPC paste was also discussed for the different preservation conditions. In all cases, changes in the transport properties (permeability, resistivity, etc.) of MKPC paste could be expected, since pore size distribution changes were observed relative to the initial pore size distributions (28 days in endogenous conditions) as well as changes in pore solution composition. Furthermore, loss of compressive strength could also be expected for MKPC pastes kept in basic solutions since a 13% increase of total porosity of MKPC paste was measured for samples kept for 6 months in pore solution of CEM V with chloride ions (Figure 12). The alkali resistance of MKPC pastes seemed to be closely related to the stability of the hydration product, K-struvite [$MgKPO_4.6H_2O$] (Figure 8, Table 11). Brucite [$Mg(OH)_2$] and Hazenite [$Mg_2KNa(PO_4)_2.14H_2O$] might precipitate as a result of K-struvite dissolution.

Acknowledgment

This work was supported by the interdisciplinary NEEDS project funded by ANDRA, CNRS, EDF, AREVA, CEA and IRSN.

References

[1] D. M. Roy, New strong cement materials: chemically bonded ceramics, Sci. 235 (1987) 651-658. https://doi.org/10.1126/science.235.4789.651

[2] A.S. Wagh, Chemically bonded phosphate ceramics, Elsevier, Amsterdam (2004) 264-267.

[3] E. Weill, J. Bradik, Magnesium phosphate cement systems, US Patent n° 4 756 762 (1988).

[4] I. Odler, Special inorganic cements, Modern concrete technology series, Taylor & Francis, London (2000) 216-224.

[5] J. Bensted, Rapid setting magnesium phosphate cement for quick repair of concrete pavements - characterization and durability aspects – Discussion, Cem. Concr. Res. 24 (1994) 595-596. https://doi.org/10.1016/0008-8846(93)90090-V

[6] Q. Yang, B. Zhu and X. Wu, Characteristics and durability test of magnesium phosphate cement-based material for rapid repair of concrete, Mater. Structures, 33 (2000) 229-234. https://doi.org/10.1007/BF02479332

[7] F. Qiao, C.K. Chau, Z. Li, Property evaluation of magnesium phosphate cement mortar as patch repair material, Constr. Build.Mater. 24 (2010) 695-700. https://doi.org/10.1016/j.conbuildmat.2009.10.039

[8] I. Buj, J. Torras, M. Rovira, J. de Pablo, Leaching behaviour of magnesium phosphate cements containing high quantities of heavy metals, J. Hazard. Mater. 175 (2010) 789-794. https://doi.org/10.1016/j.jhazmat.2009.10.077

[9] I. Buj, J. Torras, D. Casellas, M. Rovira, J. de Pablo, Effect of heavy metals and water content on the strength of magnesium phosphate cements, J. Hazard. Mater. 170 (2009) 345-350. https://doi.org/10.1016/j.jhazmat.2009.04.091

[10] S.C. Zhen, X.H. Donh, P.N. Nkrumah, Y. Su, D.K. Zhou, Effects of fly ash on the solidification / stabilization of heavy metals with magnesium phosphate cement, Int. J. Earth Sci. Engineer. 7 (2014) 1274-1279. https://doi.org/10.4028/www.scientific.net/AMR.664.683

[11] J.R. Wang, B.G. Ma, X.G. Li, H.N. Li, Z. Tian, The solidification and hydration products of magnesium phosphate cement with Pb2+, Zn2+ and Cu2+, J. Functional Mater. 45 (2014) 05060-05064. https://doi.org/10.3969/j.issn.1001-9731.2014.05.014

[12] Y. Su, J. Yang, S. Zhen, N. Lin, Y. Zhou, Solidification / stabilization of simulated cadmium-contaminated wastes with magnesium potassium phosphate cement, Environ. Engineer. Res. 21 (2016) 15-21. https://doi.org/10.4028/www.scientific.net/AMR.664.683

[13] Y. Du, M.L. Wei, K.R. Reddy, F. Jin, H.L. Wu, Z.B. Liu, New phosphate-based binder for stabilization of soils contaminated with heavy metals: leaching, strength and microstructure characterization, J. Environ. Management 146 (2014) 179-188. https://doi.org/10.1016/j.jenvman.2014.07.035

[14] X. Xu, J. Yang, Y. Gu, Properties of magnesium potassium phosphate cement containing heavy metal Pb, J. Building Mater. 19 (2016) 29-34. https://doi.org/10.3969/j.issn.1007-9629.2016.01.005

[15] A.S. Wagh, D. Singh, S.Y. Jeong, R.V. Strain, Ceramicrete stabilization of low-level mixed wastes, a complete story, Proc. 18th Annual DOE Low-Level Radioactive Waste Management Conference, Salt Lake City, UT, USA, 20-22 May (1997).

[16] A. Covill, N.C. Hyatt, J. Hill, N.C. Collier, Development of magnesium phosphate cements for radioactive waste, Adv. Applied Ceramics 110 (2011) 151-156. https://doi.org/10.1179/1743676110Y.0000000008

[17] C.A. Langton, D.B. Stefanko, M.G. Serrato, J.K. Blankenship, W.B. Griffin, J.T. Waymer, D. Matheny, D. Singh, Use of cementitious materials for SRS reactor facility in-situ decommissioning, Proc. Waste Management (WM'11) 2011 Conference, Phoenix, USA (2011).

[18] D. Singh, A.S. Wagh, M. Tlustochowicz, S.Y. Jeong, Phosphate ceramic process for macroencapsulation and stabilization of low-level debris wastes, Waste Management 18 (1998) 135-143. https://doi.org/10.1016/S0956-053X(98)00018-X

[19] C. Cau-Dit-Coumes, D. Lambertin, H. Lahalle, P. Antonucci, C. Cannes, S. Delpech, Selection of a mineral binder with potentialities for the stabilization / solidification of aluminum metal, J. Nucl. Mater. 453 (2014) 31-40. https://doi.org/10.1016/j.jnucmat.2014.06.032

[20] A.S. Wagh, S.Y. Sayenko, V.A. Shkuropatenko, R.V. Tarasov, M.P. Dykiy, Y.O. Svitlychniy, V.D. Virych, E.A. Ulybkina, Experimental study on caesium immobilization in struvite structures, J. Hazard. Mater. 302 (2016) 241-249. https://doi.org/10.1016/j.jhazmat.2015.09.049

[21] G. Mestres, M.P. Ginebra, Novel magnesium phosphate cements with high early strength and antibacterial properties, ActaBiomaterialia 7 (2011) 1853-1861. https://doi.org/10.1016/j.actbio.2010.12.008

[22] G. Mestres, M. Abdolhosseini, W. Bowles, S.-H.Huang, C. Aparicio, S.-U.Gorr, M.-P.Ginebra, Antimicrobial properties and dentin bonding strength of magnesium phosphate cements, Acta Biomaterialia 9 (2013) 8384-8393. https://doi.org/10.1016/j.actbio.2013.05.032

[23] H. Zhou, A.K. Agarwal, V.K. Goel, S.B. Bhaduri, Microwave assisted preparation of magnesium phosphate cement (MPC) for orthopedic applications: A novel solution to the exothermicity problem, Materials Science and Engineering: C 33 (2013) 4288-4294. https://doi.org/10.1016/j.msec.2013.06.034

[24] C.K. Chau, F. Qiao, Z. Li, Potentiometric study of the formation of magnesium potassium phosphate hexahydrate, J. Mater. Civ. Eng. 24 (2012) 586–591. https://doi.org/10.1061/(ASCE)MT.1943-5533.0000410

[25] S. Zhen, X. Dong, G. Appiah-Sefah, M. Pan, D. Zhou, Analysis of changes in hydration products during solidification/stabilization process of heavy metals in the presence of magnesium potassium phosphate cement, J. Applied Sci. Engineer. 17 (2014) 413-421. https://doi.org/10.6180/jase.2014.17.4.08

[26] H. Lahalle, C. Cau-Dit-Coumes, A. Mesbah, D. Lambertin, C. Cannes, S. Delpech, S. Gauffinet, Investigation of magnesium phosphate cement hydration in diluted suspension and its retardation by boric acid, Cement and Concrete Research Journal. 87 (2016) 77-86. https://doi.org/10.1016/j.cemconres.2016.04.010

[27] A. Viani, M. Peréz-Esteban, S. Pollastri, A. F. Gualtieri, In situ synchrotron powder diffraction study of the setting reaction kinetics of magnesium-potassium phosphate cements, Cem. Concr. Res. 79 (2016) 344-352. https://doi.org/10.1016/j.cemconres.2015.10.007

[28] M. Le Rouzic, T. Chaussadent, G. Platret, L. Stefan, Mechanisms of k-struvite formation in magnesium phosphate cements, Cement and Concrete Research Journal. 91 (2017) 117-122. https://doi.org/10.1016/j.cemconres.2016.11.008

[29] H. Lahalle, C. Cau-Dit-Coumes, C. Mercier, D. Lambertin, C. Cannes, S. Delpech, S. Gauffinet, Influence of the w/c ratio on the hydration process of a magnesium phosphate cement and its

retardation by boric acid, Cement and Concrete Research Journal. 109 (2018) 159-174. https://doi.org/10.1016/j.cemconres.2018.04.010

[30] N. Yang, C. Shi, J. Yang, Y. Chang, Research progresses in magnesium phosphate cement-based materials (review), J. Mater. Civil Engineer. 26 (2014) article n°04014071. https://doi.org/10.1061/(ASCE)MT.1943-5533.0000971

[31] B. Xu, H. Ma, Z. Li, Influence of magnesia-to-phosphate molar ratio on microstructures, mechanical properties and thermal conductivity of magnesium potassium phosphate cement paste with large water-to-solid ratio, Cement and Concrete Research Journal. 68 (2015) 1-9. https://doi.org/10.1016/j.cemconres.2014.10.019

[32] Z.Q. Qi, H.T. Wang, J.H. Ding, S.H Zhang, Study on the drying shrinkage property of magnesium phosphate cement, Mater. Science Forum 852 (2016) 1468-1472. https://doi.org/10.4028/www.scientific.net/MSF.852.1468

[33] M. Le Rouzic, T. Chaussadent, L. Stefan, M. Saillio, On the influence of Mg/P ratio on the properties and durability of magnesium potassium phosphate cement pastes, Cem. Concr. Res. 96 (2017) 27-41. https://doi.org/10.1016/j.cemconres.2017.02.033

[34] A.J. Wang, Z.L. Yuan, J.Zhang, L.T. Liu, J.M. Li, Z.Liu, Effect of raw material ratios on the compressive strength of magnesium potassium phosphate chemically bonded ceramics, Mater. Sci. Engineer. C 33 (2013) 5058-5063. https://doi.org/10.1016/j.msec.2013.08.031

[35] R.Q. Liu, D.Q. Chen, T.B. Hou, Study on preparation and setting time of magnesium potassium phosphate cement, Adv. Mater. Res. 1049 (2014) 251-255. https://doi.org/10.4028/www.scientific.net/AMR.1049-1050.251

[36] H. Ma, B. Xu, J. Liu, H. Pei, Z. Li, Effects of water content, magnesia-to-phosphate molar ratio and age on pore structure, strength and permeability of magnesium potassium phosphate cement paste, Mater. Design 64 (2014) 497-502. https://doi.org/10.1016/j.matdes.2014.07.073

[37] Y. Li, J. Sun, B. Chen, Experimental study of magnesia and M/P ratio influencing properties of magnesium phosphate cement, Construction Build. Mater. 65 (2014) 177-183. https://doi.org/10.1016/j.conbuildmat.2014.04.136

[38] H. Ma, B. Xu, Potential to design magnesium potassium phosphate cement paste based on an optimal magnesia-to-phosphate ratio, Mater. Design 118 (2017) 81-88. https://doi.org/10.1016/j.matdes.2017.01.012

[39] Q. Yang, B. Zhu, X. Wu, Characteristics and durability test of magnesium phosphate cement-based material for rapid repair of concrete. Mater.Struct. 33 (2000) 229-234. https://doi.org/10.1007/BF02479332

[40] Y. Li, B. Chen, Factors that affect the properties of magnesium phosphate cement, Constr. Build, Mater. 47 (2013) 977-983. https://doi.org/10.1016/j.conbuildmat.2013.05.103

[41] H. Wang, M. Xue, J. Cao, Research on the Durability of Magnesium Phosphate Cement, Advanced Materials Research, 168-170 (2011) 1864-1868. https://doi.org/10.4028/www.scientific.net/AMR.168-170.1864

[42] M. Le Rouzic, T. Chaussadent, L. Stefan, M. Saillio, On the influence of Mg/P ratio on the properties and durability of magnesium potassium phosphate cement pastes, Cement and Concrete Research, 96 (2017) 27-41. https://doi.org/10.1016/j.cemconres.2017.02.033

[43] D.V. Ribeiro, J.A.M. Agnlei, M.R. Morelli, Study of mechanical properties and durability of magnesium phosphate cement matrix containing grinding dust, Mater. Res., 16 (5) (2013) 1113-1121. http://dx.doi.org/10.1590/S1516-14392013005000105

[44] S. Chattopadhyay, Evaluation of Chemically Bonded Phosphate Ceramics for a Mercury Stabilization of a Mixed Synthetic Waste, 2003 (EPA/600/R-03/113). https://clu-in.org/download/contaminantfocus/mercury/EPA_phosphateceramics.pdf

[45] M. Xue, H. Wang, X. Xiao, J. Cao, Influence of m(P)/m(M) mass ratio on properties of magnesium phosphate cement and its mechanism analysis, J. Functional Mater. 46 (2015) 23090-23095.

[46] P.K. Mehta, Magnesium oxide additive for producing self-stress in mass concrete, Proc. 7th Intern. Congress on the Chemistry of Cement, Paris, France, 3 (1980) 6-9.

[47] A.H. White, Volume changes of Portland cement as affected by chemical composition and ageing, Proc. American Society for Testing and Materials 28 (1928) 398-431.

[48] J. Rodriguez-Carvajal, FULLPROF: a program for Rietveld refinement and pattern matching analysis, in satellite meeting on powder diffraction of the XV congress of IUCr, 1990, Toulouse, France.

[49] S. Graeser, W. Postl, H.P Bojar, P. Berlepsch, T. Armbruster, T. Raber, K. Ettinger, F. Walter, Struvite-(K), $KMgPO_4 \cdot 6(H_2O)$, the potassium equivalent of struvite – a new mineral, European Journal of Mineralogy, 20 (2008) 629-633. https://doi.org/10.1127/0935-1221/2008/0020-1810

[50] G. Brunauer, H.Boysen, F. Frey, T. Hansen, W. Kriven, 'High temperature crystal structure of a 3:2 mullite from neutron diffraction data', ZeitschriftfuerKristallographie', 216 (2001) 284-290. https://doi.org/10.1524/zkri.216.5.284.20375

[51] H. Amour, W. Denner, H. Schulz, 'Structure determination of alpha-quartz up to $68*10^8$ Pa', Acta Crystallographica B, 35 (1979) 550-555. https://doi.org/10.1107/S056774087900412X

[52] V.G. Tsirel'son, A.S. Avilov, Yu. A. Abramov, D. Feil, X-ray and electron diffraction study of MgO, Acta Crystallographica, Section B: Structural Science, 54 (1998) 8-17. https://doi.org/10.1107/S0108768197008963

[53] J.R. Holden, C.W. Dickinson, Crystal structures of three solid solution phases of potassium nitrate and ammonium nitrate, Journal of Physical Chemistry, 79 (1975) 249-256. https://doi.org/10.1021/j100570a011

[54] C. Gallé, Effect of drying on cement-based materials pore structure as identified by mercury intrusion porosimetry: A comparative study between oven-, vacuum-, and freeze-drying, Cement and Concrete Research, 31(10) (2001) 1467-1477. https://doi.org/10.1016/S0008-8846(01)00594-4

[55] M. Moukwa, P.C. Aitcin, The effect of drying on cement pastes pore structure as determine by mercury prosimetry, Cement and Concrete Research, 18 (1988) 745-752. https://doi.org/10.1016/0008-8846(88)90098-1

[56] F. Moro, H. Böhni, Ink-Bottle Effect in Mercury Intrusion Porosimetry of Cement Based Materials, Journal of Colloid and Interface Science, 246(1) (2002) 135-149. https://doi.org/10.1006/jcis.2001.7962

[57] J. Rouquerol, D. Avnir, C.W. Fairbridge, D. H. Everett, J. M. Haynes, N. Pernicone, J. D. F. Ramsay, K.S.W. Sing, K.K. Unger, Recommendations for the characterization of porous solids (Technical Report), Pure Appl. Chem., 66 (8) (1994). https://doi.org/10.1515/iupac.66.0925

[58] M. Cyr, P. Rivard, F. Labrecque, A. Daidié, High-pressure device for fluid extraction from porous materials: application to cement-based materials, Journal of the American Ceramic Society, 91 (2008) 2653-2658. https://doi.org/10.1111/j.1551-2916.2008.02525.x

[59] M. Mathew and E.D. Schroeder, Crystal structure of struvite analogue $MgKPO_4.6H_2O$. Acta Crystallographica, B.35 (1979) 11-13. https://doi.org/10.1107/S0567740879002429

[60] S. Zhang, H.-S. Shi, S.-W. Huan, and P. Zhang, Dehydration characteristics of struvite-K pertaining to magnesium potassium phosphate cement system in non-isothermal condition, Journal of Thermal Analysis and Calorimetry, 111: 1 (2013) 35-40. https://doi.org/10.1007/s10973-011-2170-9

[61] L.J. Gardner, S.A. Bernal, S.A. Walling, C.L. Corkhill, J.L. Provis, N.C. Hyatt, Characterization of magnesium potassium phosphate cements blended with fly ash and ground granulated blast furnace slag, Cement and Concrete Research, 74 (2015) 78-87. https://doi.org/10.1016/j.cemconres.2015.01.015

[62] B. Xu, H. Ma, H. Shao, Z. Li, B. Lothenbach, Influence of fly ash on compressive strength and micro-characteristics of magnesium potassium phosphate cement mortars, Cement and Concrete Research, 99 (2017) 86-94. https://doi.org/10.1016/j.cemconres.2017.05.008

[63] T. Yoshida, T. Tanaka, H. Yoshida, T. Funabiki, and S. Yoshida, Study of dehydration of magnesium hydroxide, The Journal of Physical Chemistry, 99: 27 (1995) 10890-10896. https://doi.org/10.1021/j100027a033

[64] R.C. Turner, I. Hoffman, and D. Chen, Thermogravimetry of the dehydration of Mg(OH)2, Canada Department of Agriculture, Ottawa (1992). https://doi.org/10.1139/v63-039

[65] He. Yang, H.J Sun, R.T. Downs, Hazenite, $KNaMg_2(PO_4)_2.14H2O$, a new biologically related phosphate mineral, from Mono Lake, California, USA, American Mineralogist,96 (2011) 675-681.

[66] C.K. Chauhan, M.J. Joshi, Growth and characterization of struvite-Na crystals. Journal of Crystal Growth, 401 (2014) 221-226. https://doi.org/10.1002/crat.201000587

[67] F.-Y. Ma, Corrosive Effects of Chlorides on Metals, Pitting Corrosion, Prof. Nasr Bensalah (Ed.), ISBN: 978-953-51-0275-5 (2012), InTech. http://cdn.intechopen.com/pdfs/33625/intech-corrosive_effects_of_chlorides_on_metals.pdf

[68] J.E. Gillott, Alkali-aggregate reactions in concrete, Engineering Geology, 9: 4 (1975) 303-326.

[69] J.A. Larbi, P.P. Hudec, A study of alkali-aggregate reaction in concrete: Measurement and prevention: Part I: Measurement – Development of rapid ar test method, Cement and Concrete Research, 19: 6 (1989), 905-912. https://doi.org/10.1016/0008-8846(89)90103-8

[70] T. Zhang, H. Chen, X. Li, Z. Zhu, Hydration behavior of magnesium potassium phosphate cement and stability analysis of its hydration products through thermodynamic modeling, Cem. Concr. Res. 98 (2017) 101-110. https://doi.org/10.1016/j.cemconres.2017.03.015

[71] A.M. Benet, Potential for potassium recovery as K-struvite, PhD Thesis, University of British Columbia (Vancouver), 2015. https://doi.org/10.14288/1.0166487